2017 Fall

"Phase Transformation *in* Materials"

11.10.2017

Eun Soo Park

Office: 33-313
Telephone: 880-7221
Email: espark@snu.ac.kr
Office hours: by an appointment

Chapter 3 Crystal Interfaces and Microstructure

1) Interfacial Free Energy

2) Solid/Vapor Interfaces

3) Boundaries in Single-Phase Solids

4) Interphase Interfaces in Solid (α/β)

5) Interface migration

Contents for previous class

Chapter 3 Crystal Interfaces and Microstructure

1) Interfacial Free Energy (γ : J/m^2)

→ The Gibbs free energy of a system containing an interface of area A

→ $G_{bulk} + G_{interface}$ vapor / solid $G = G_0 + \gamma A$ → $F = \gamma + A\, d\gamma/dA$ (liq. : $d\gamma/dA = 0$)

* Origin of the surface free energy (E_{SV})? → Broken Bonds

$high\ T_m \rightarrow high\ L_s \rightarrow high\ \gamma_{sv}$

2) Solid/Vapor Interfaces

* γ interfacial energy = free energy (J/m^2)

→ $\gamma = G = H - TS$

$= E + PV - TS$ (: PV is ignored)

→ $\gamma = E_{sv} - TS_{sv}$ (S_{sv} thermal entropy, configurational entropy)

→ $\partial\gamma/\partial T = -S$: surface energy decreases with increasing T

γ-θ plot

Equilibrium shape: Wulff surface

$$\sum_{i=1}^{n} A_i \gamma_j = Minimum$$

$E_{SV} = 3\,\varepsilon/2 = 0.25\, L_S / N_a$ ⇨ $\gamma_{SV} = 0.15\, L_S / N_a$ J / surface atom

(∵ surface free Es averaged over many surface plane, S effect at high T)

Surface energy for high or irrational {hkl} index

(cosθ/a)(1/a) : **broken bonds from the atoms on the steps**

(sin|θ|/a)(1/a) : **additional broken bonds from the atoms on the steps**

Attributing ε/2 energy to each broken bond,

$$E_{SV} = \frac{1}{1\times a}\frac{\varepsilon}{2}\left(\frac{\cos\theta}{a}+\frac{\sin|\theta|}{a}\right)$$

$$= \frac{\varepsilon\left(\cos\theta+\sin\left(|\theta|\right)\right)}{2a^2}$$

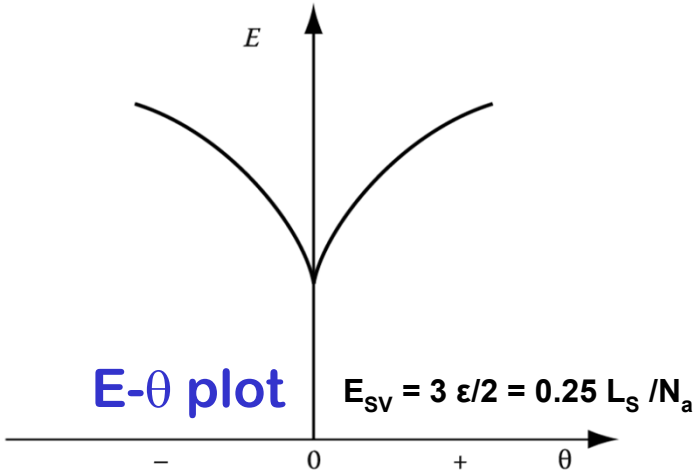

Fig. 3.4 Variation of surface energy as a function of θ

- **The close-packed orientation (θ = 0) lies at a cusped minimum in the E plot.**
- **Similar arguments can be applied to any crystal structure for rotations about any axis from any reasonably close-packed plane.**
- **All low-index planes should therefore be located at low-energy cusps.**
- **If γ is plotted versus θ similar cusps are found (γ-θ plot), but as a result of entropy effects they are less prominent than in the E-θ plot, and for the higher index planes they can even disappear.**

Equilibrium shape: Wulff surface

* A convenient method for plotting the variation of γ with surface orientation in 3 dimensions

* Distance from center : γ_{sv}

→ Construct the surface using γ_{sv} value as a distance between the surface and the origin when measured along the normal to the plane

Several plane A_1, A_2 etc. with energy γ_1 , γ_2

Total surface energy : $A_1\gamma_1 + A_2\gamma_2 \ldots$

$= \sum A_i \gamma_i \rightarrow$ minimum

→ equilibrium morphology

: can predict the equilibrium shape of an isolated single crystal

How is the equilibrium shape determined?

$$\sum_{i=1}^{n} A_i \gamma_j = Minimum$$

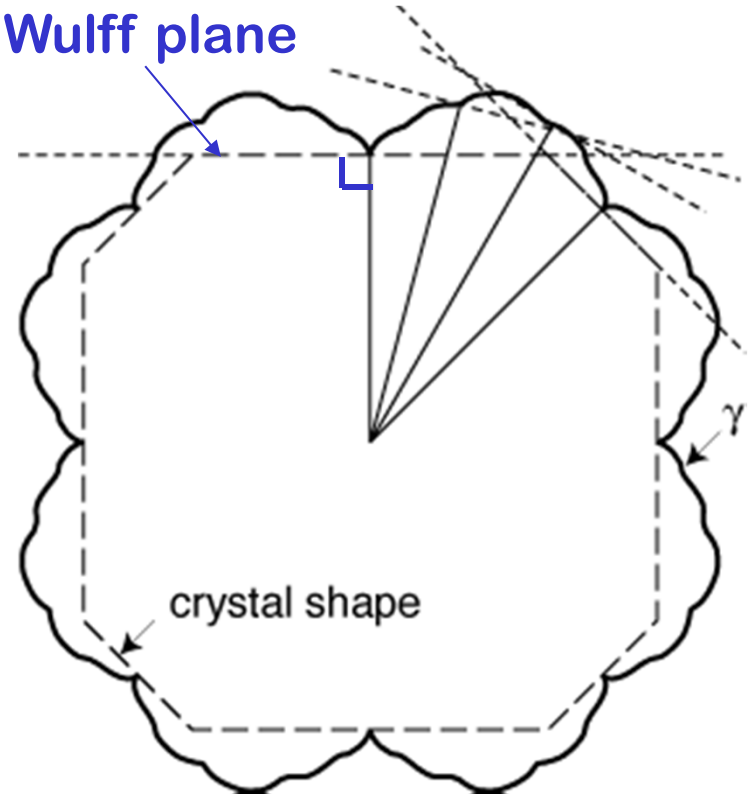

γ-θ plot

Due to entropy effects the plot are less prominent than in the E_{SV}-θ plot, and for the higher index planes they can even disappear

Contents for previous class

3) Boundaries in Single-Phase Solids

(a) Low-Angle and High-Angle Boundaries

Θ < 15° : total energy of the dislocations within unit area of boundary

Θ > 15° : impossible to physically identify the individual dislocations → strain field overlap → cancel out

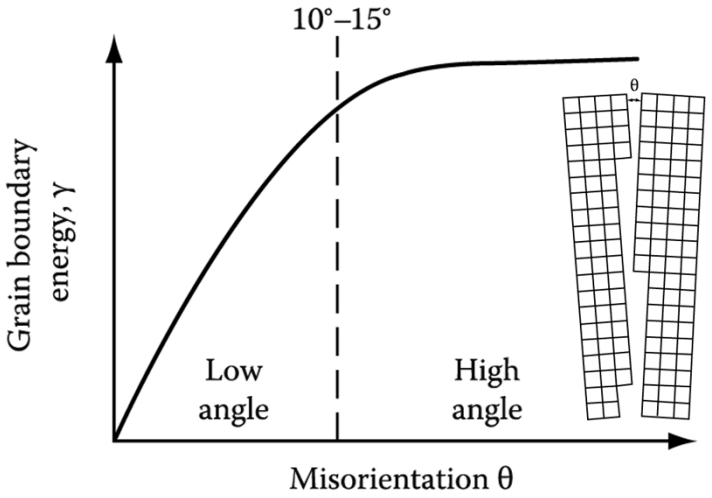

Broken Bonds → high angle $\gamma_{g.b.} \approx 1/3\ \gamma_{S/V.}$

(b) Special High-Angle Grain Boundaries

: high angle boundary but with low $\gamma_{g.b.}$

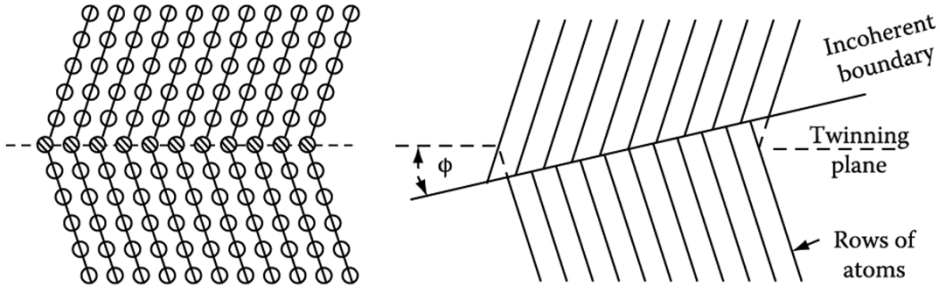

→ twin boundary

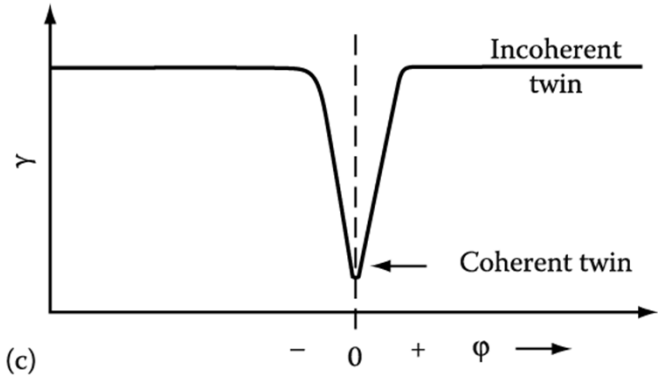

Atoms in the boundary are essentially in undistorted positions ~relatively little free volume

(c) Equilibrium in Polycrystalline Materials

Metastable equilibrium at the GB intersections (Balances of 1) boundary E + 2) surface tension)

- **Thermally Activated Migration of Grain Boundaries:**

→ real curvature (ΔP → ΔG: Gibbs Thomson Eq.) → $F = 2\gamma/r = \Delta G/V_m$ (by curvature)
(Pulling force per unit area of boundary)

→ Grain coarsening at high T annealing

- **Kinetics of Grain Growth**

- Grain boundary migration (v) by thermally activated atomic jump

Boundary velocity $v = \frac{A_2 n_1 v_1 V_m^{\,2}}{N_a RT} \exp\left(-\frac{\Delta G^a}{RT}\right) \frac{\Delta G}{V_m}$

$v \sim \Delta G/V_m$ driving force

→ $F = \Delta G/V_m$

M : mobility = velocity under unit driving force ~ exp (-1/T)

rate of grain growth $dD/dt \sim 1/D$, exponentially increase with T

→ $D = k't^n$

(Experimental: n << 1/2, ½ at pure metals or high Temp.)

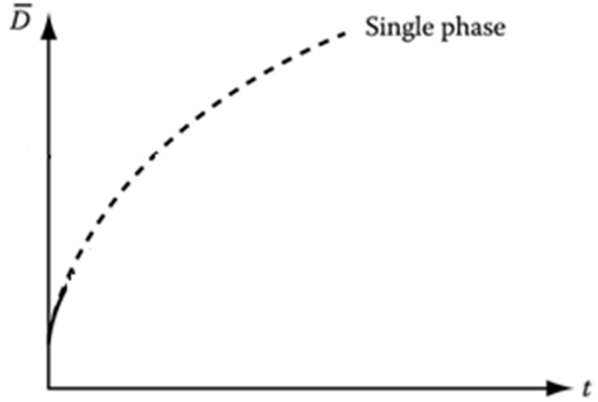

Normal Grain Growth

- Grain boundary moves to reduce area and total energy
- Large grain grow, small grains shrink
- Average grain size increases
- Little change of size distribution

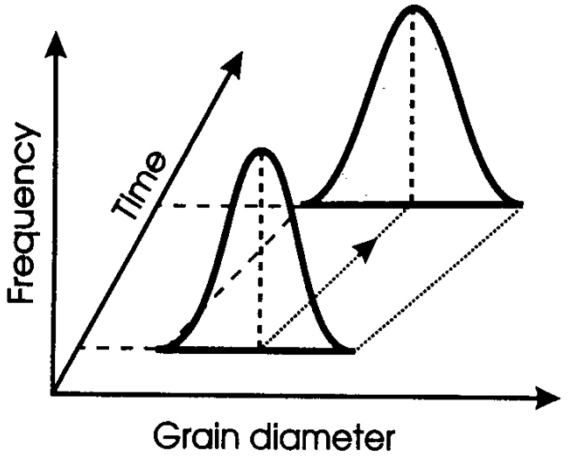

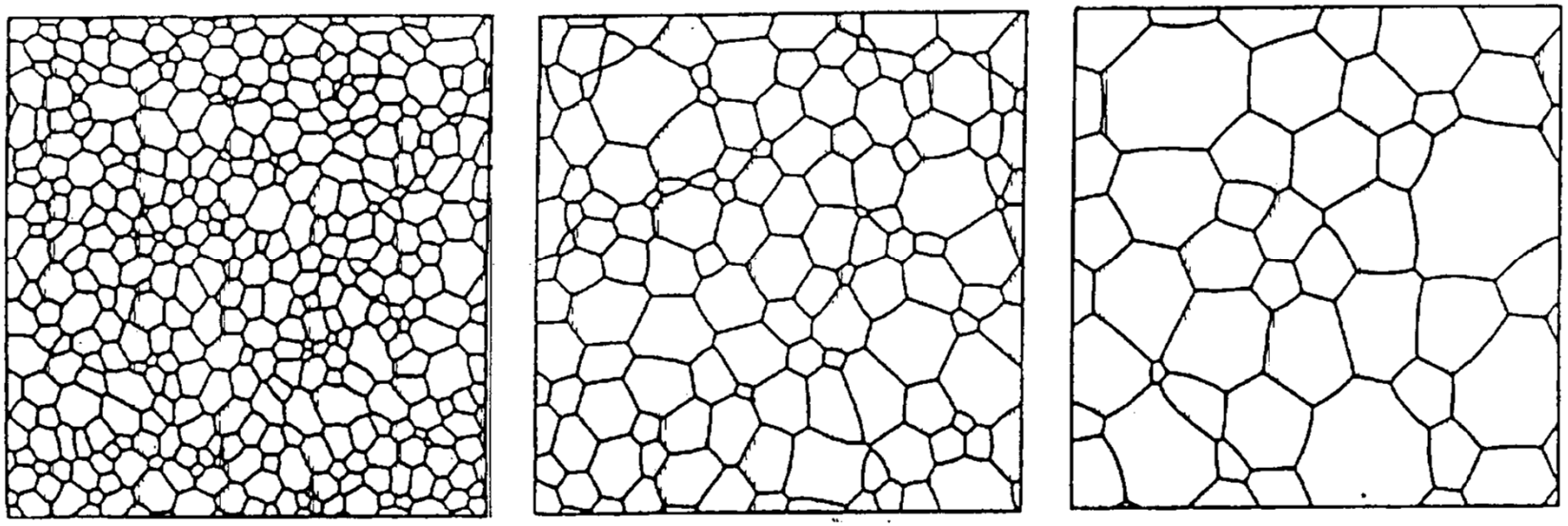

Ref. Hillert ACTA Mater. 13 227 (1965)

Considering factors of G.B. growth

(a) Impurity (solute) drag

(b) Pinning particle

(c) 2^{nd} phases

(d) Anisotropic σ, M

(e) Strain energy

(f) Free surface

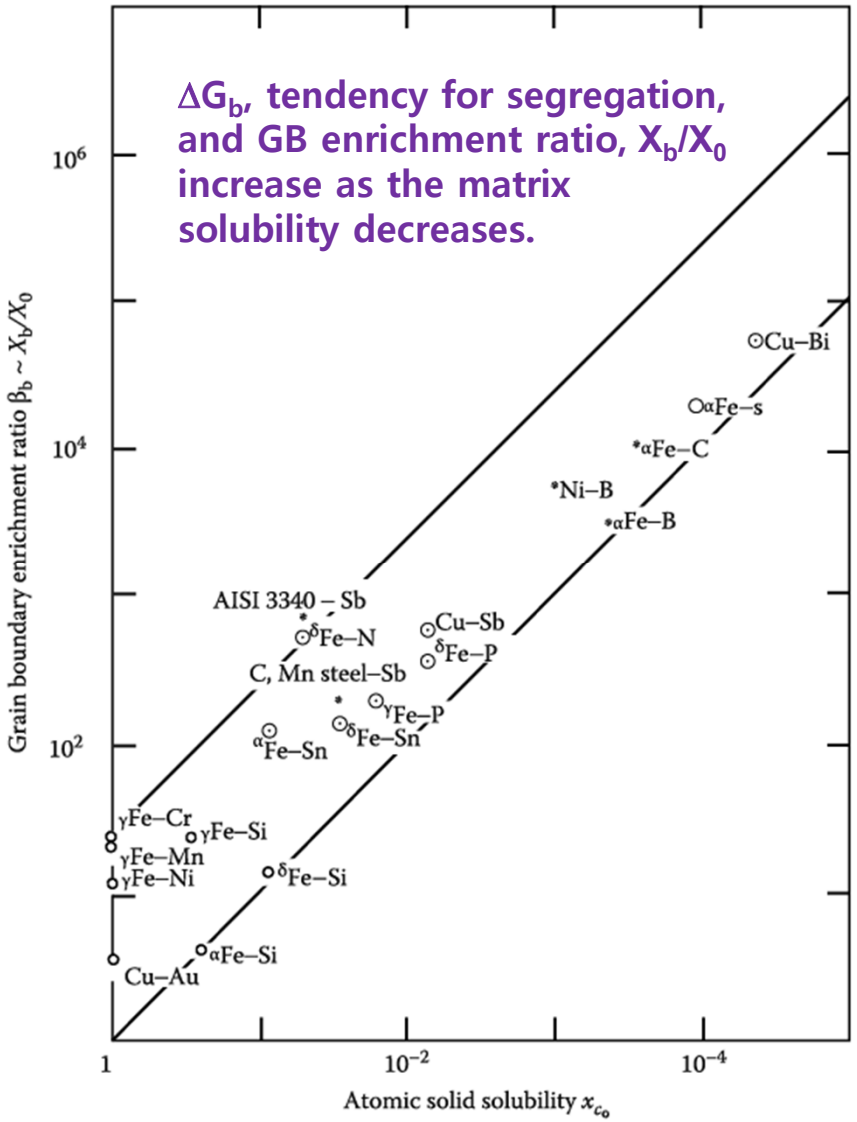

<Increasing GB enrichment with decreasing solid solubility in a range of system>

(a) Impurity (solute) drag

* Solute drag effect

In general,
G_b (grain boundary E) and mobility of pure metal decreases on alloying.

~Impurities tend to stay at the GB.

Generally, ΔG_b, tendency of segregation, increases as the matrix solubility decreases.

$$X_b = X_0 \exp \frac{\Delta G_b}{RT}$$

X_b/X_0: GB enrichment ratio

- Decreases as temp. increases, i.e., the solute "evaporates" into the matrix

Low T or ΔG_b ⇧ X_b ⇧ Mobility of G.B. ⇩

→ Alloying elements affects mobility of G.B.

X_0 : matrix solute concentration/ X_b : boundary solute concentration

ΔG_b : free energy reduced when one mole of solute is moved to GB from matrix.

(ΔG_b) → The high mobility of special boundaries can possibly be attributed to a low solute drag on account of the relatively more close-packed structure of the special boundaries.

(b) Pinning particle or (c) 2nd phases

Schematic diagram illustrating the possible interactions of second phase particles and migrating grain boundaries.

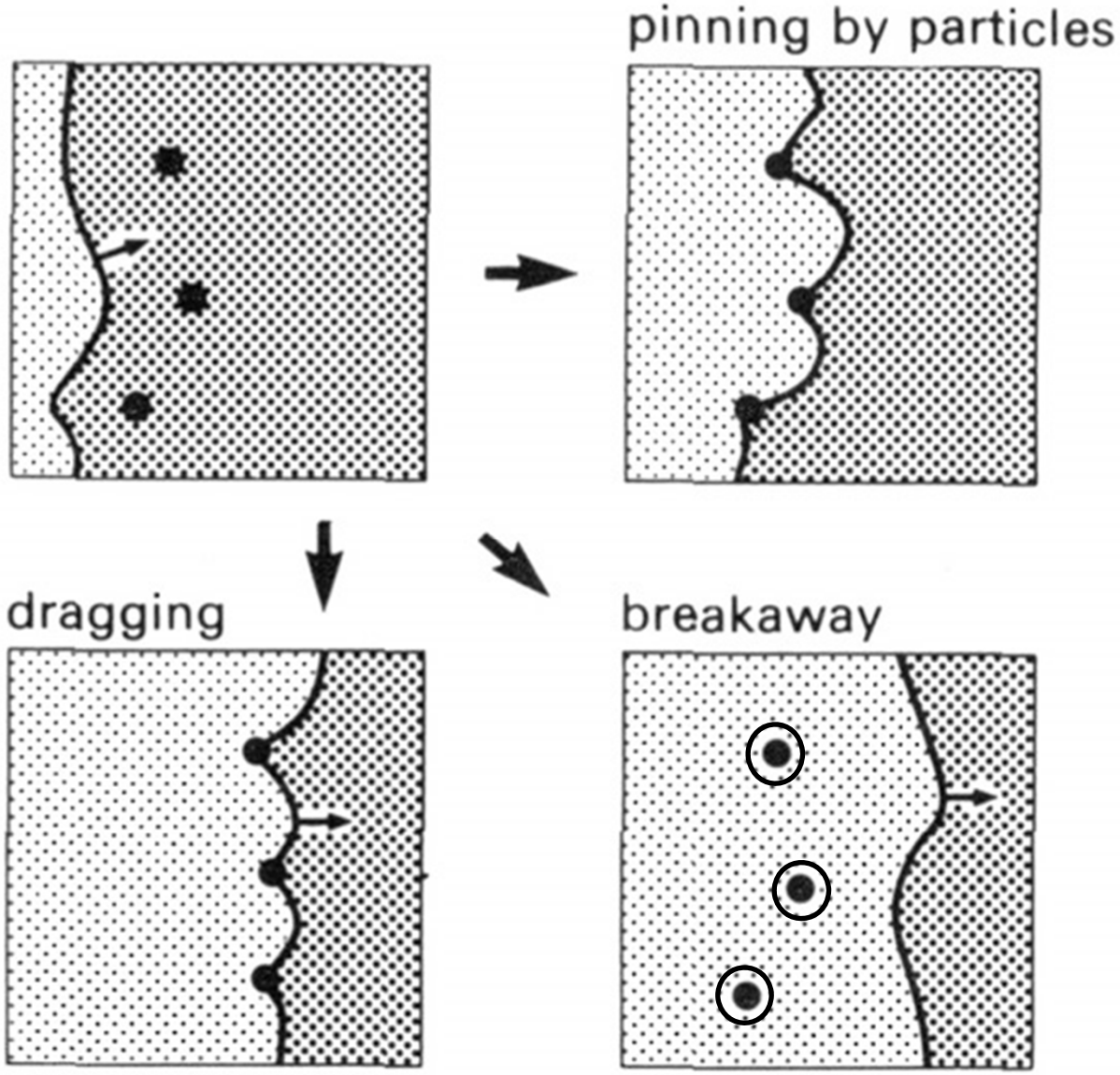

Interaction with particles

Zener Pinning

$$P = \frac{3f_v}{2\pi r^2} \cdot \pi r \gamma = \frac{3f_v \gamma}{2r}$$

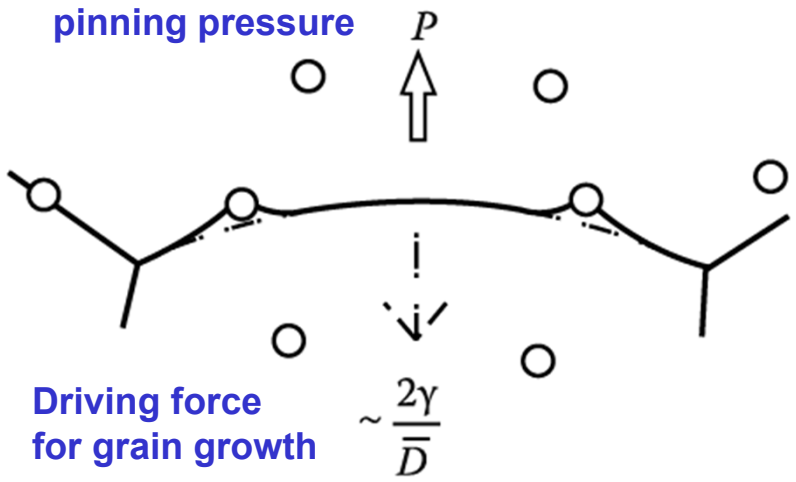

→ F = 2γ/r = ΔG/V_m (by curvature)

This force will oppose the driving force for grain growth, $2\gamma/\bar{D}$.

$$\frac{2\gamma}{\bar{D}} = \frac{3f_v\gamma}{2r} \rightarrow \bar{D}_{max} = \frac{4r}{3f_v}$$

Driving force will be insufficient to overcome the drag of the particles and grain growth stagnates.

For fine grain size
→ a large volume fraction of very small particles

* Effect of second-phase particles on grain growth

$$\bar{D}_{max} = \frac{4r}{3f_v}$$

: Stabilization of a fine grain size during heating at high temp. → large volume fraction (f ↑) of very small particles (r ↓).

$$\bar{D}_{max} = \frac{4r}{3f_v} \downarrow$$

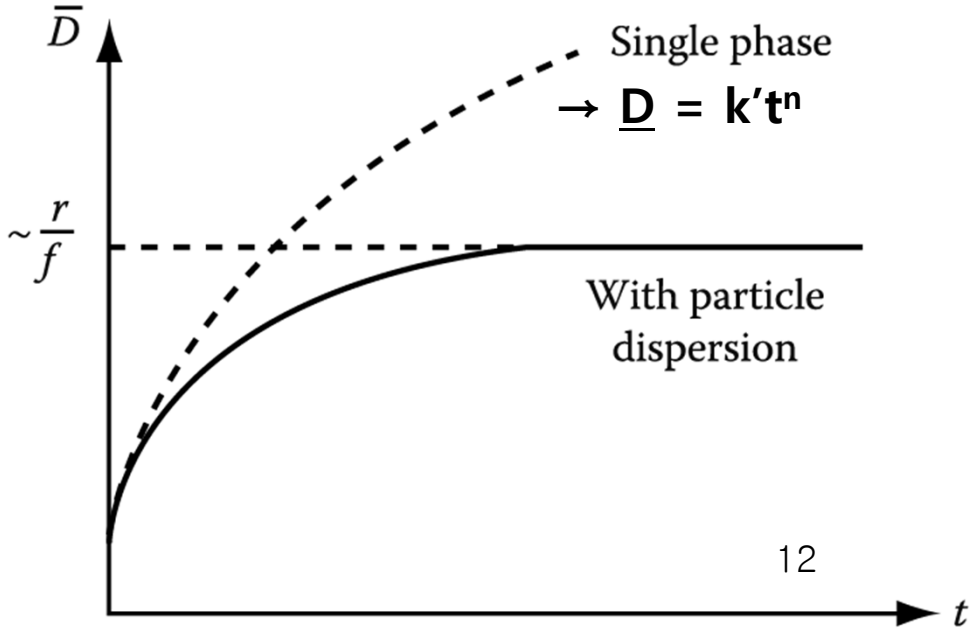

Abnormal Grain Growth

(high mobility of special GBs → development of recrystallization textures)

❑ **Discontinuous grain growth of a few selected grains**

- Local breaking of pinning by precipitates
- Anisotropy of grain boundary mobility
- Anisotropy of surface & grain boundary energy
- Selective segregation of impurity atoms
- Inhomogeneity of strain energy

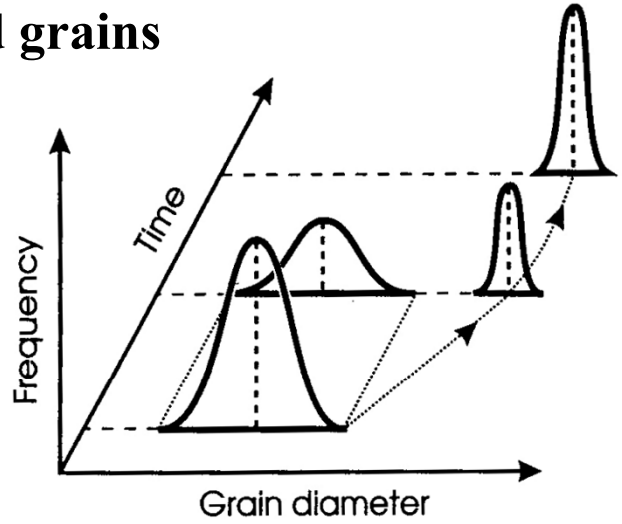

❑ **Bimodal Size distribution**

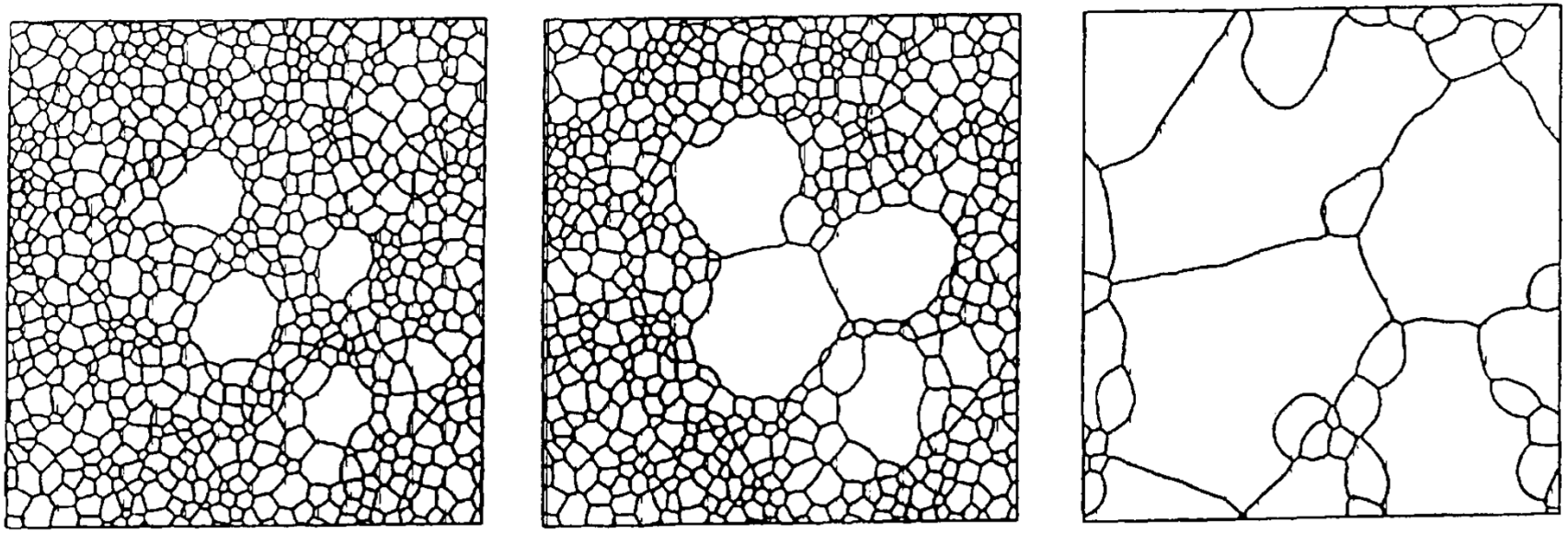

- **Grain Growth**

  - Normal grain growth ⟺ Abnormal grain growth

    (high mobility of special GBs
    → development of recrystallization textures)

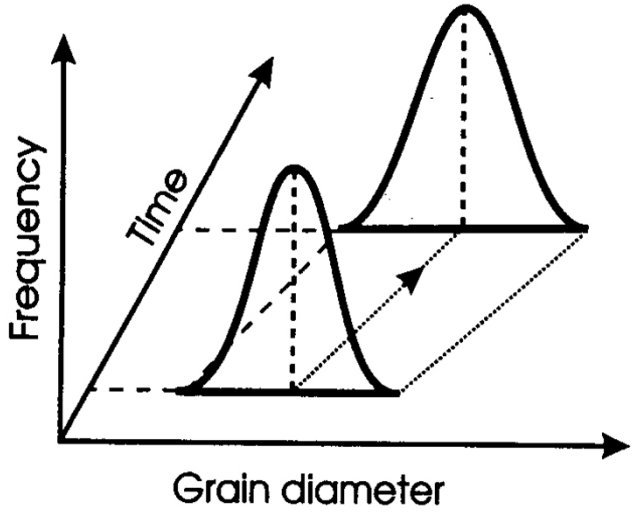

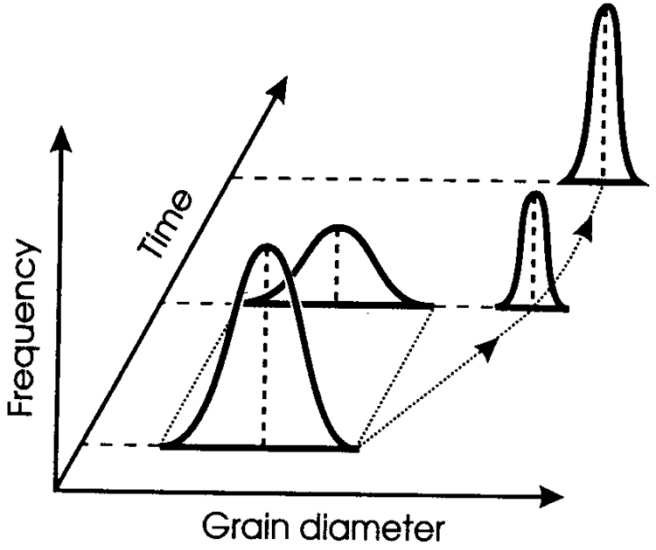

< Bimodal Size distribution >

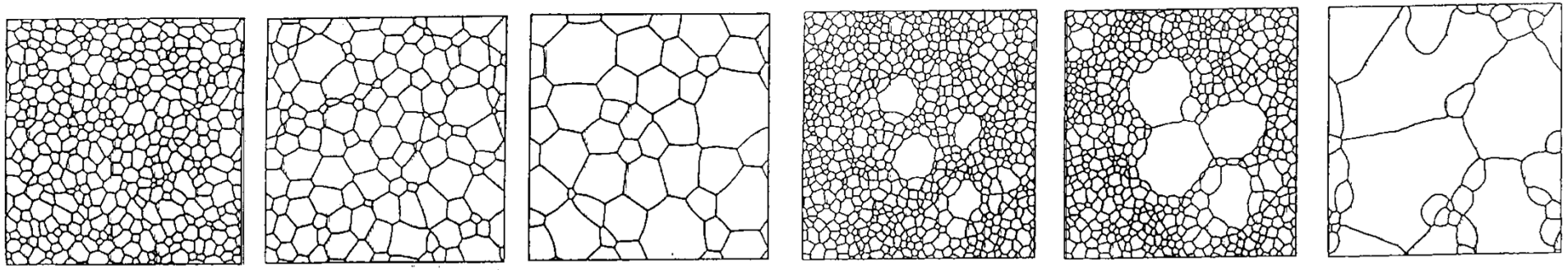

Contents for today's class

- **Interphase Interfaces in Solid (α/β)**

  - Types of interphase interfaces in solid (α/β)

  - Second-Phase Shape

    $$\sum A_i \gamma_i + \Delta G_S = minimum$$

    - Interface Energy Effects
      - Coherent / Semi-coherent / incoherent
    - Misfit Strain Effects

  - Coherency Loss

  - Glissil Interfaces ⟺ Solid/Liquid Interfaces

- **Interface migration**

  - Interface controlled growth ⟺ Diffusion controlled growth

Q: What kind of interphase interfaces in solid (α/β) exist?

= coherent/ semi-coherent / incoherent/ complex semi-coherent

→ different interfacial free energy, γ

3.4 Interphase Interfaces in Solids

Interphase boundary
- different two phases : different crystal structure
different composition

{ **coherent,**
semicoherent
incoherent

3.4.1 Coherent interfaces

Disregarding chemical species, if the interfacial plane has the same atomic configuration in both phases,

Perfect atomic matching at interface

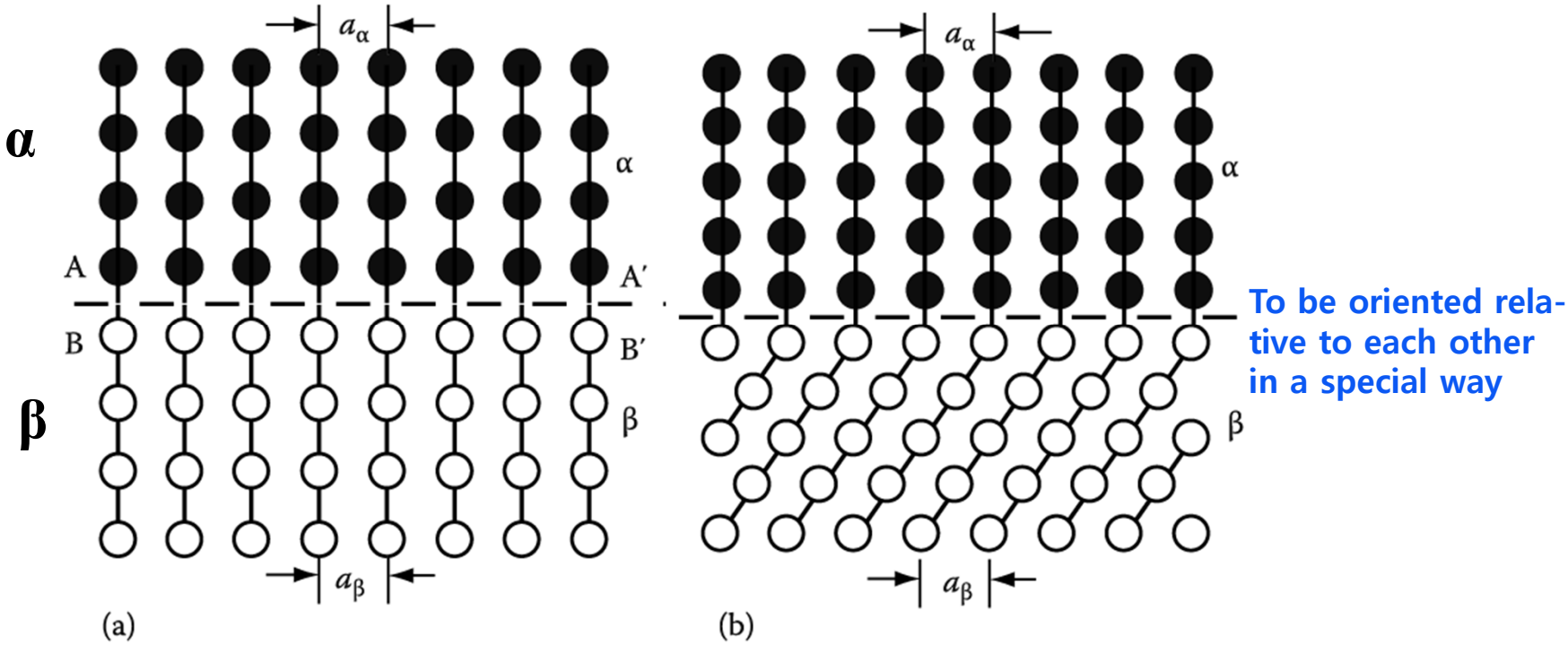

Fig. 3.32 Strain-free coherent interfaces. (a) Each crystal has a different chemical composition but the same crystal structure. (b) The two phases have different lattices

3.4.1 Coherent interfaces

Which plane and direction will be coherent between FCC and HCP?

: **Interphase interface will make lowest energy and thereby the lowest nucleation barrier**

ex) hcp silicon-rich κ phase in fcc copper-rich α matrix of Cu-Si alloy

→ the same atomic configuration
& interatomic distance

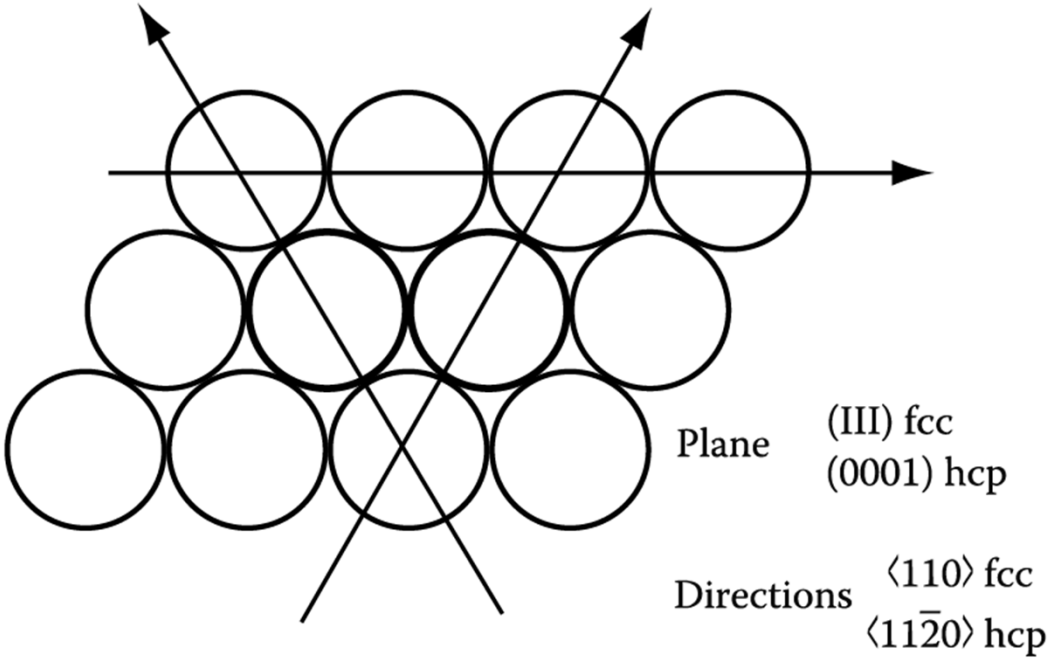

Fig. 3.33 **The close-packed plane and directions in fcc and hcp structures**.

→ Orientation relation

Cu $(111)_\alpha // (0001)_\kappa$ Si

$[\bar{1}10]_\alpha // [11\bar{2}0]_\kappa$

$\gamma_{\alpha\text{-}\kappa}$ of Cu-Si ~ 1 mJm^{-2}

In general,
γ (coherent) ~ 200 mJm^{-2}

$\gamma_{coherent} = \gamma_{structure} + \gamma_{chemical}$

$= \gamma_{chemical}$

γ (coherent) = γ_{ch}

hcp/ fcc interface: only one plane that can form a coherent interface

When the atomic spacing in the interface is not identical between the adjacent phase, what would happen?

Possible to maintain coherency by straining one or both crystal lattices.

→ lattice distortion

→ Coherency strain

→ strain energy

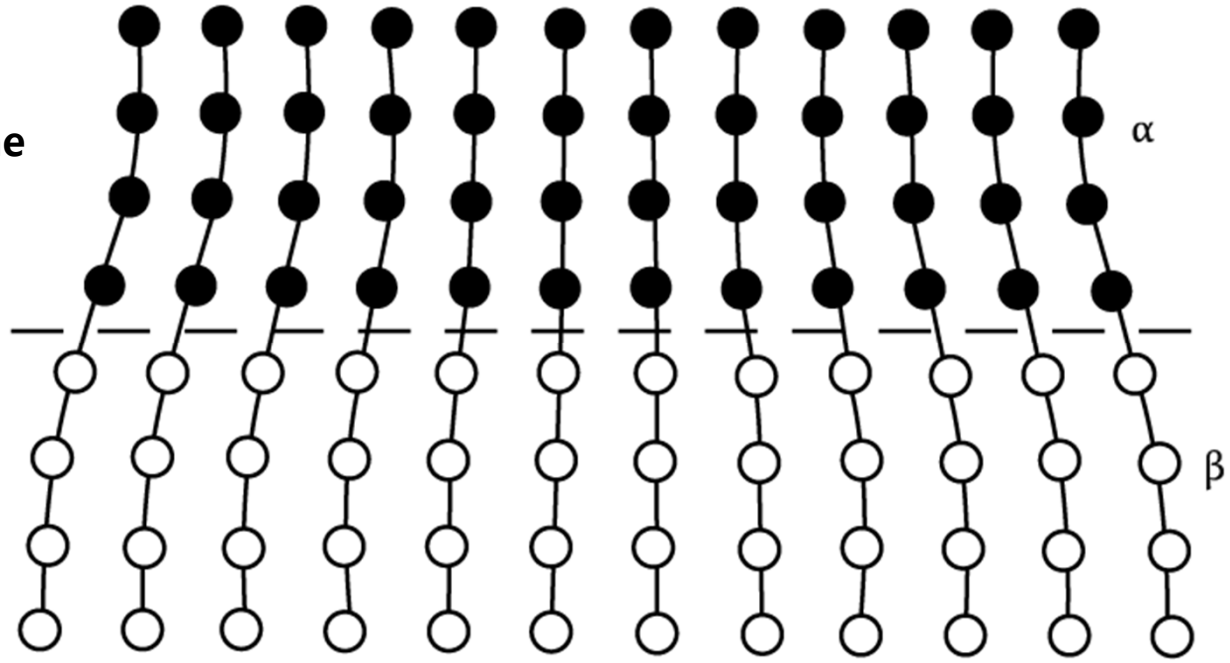

Fig. 3.34 A coherent interface with slight mismatch leads to coherency strains in the adjoining lattices.

The strains associated with a coherent interface raise the total energy of the system.

How can this coherent strain can be reduced?

If coherency strain energy is sufficiently large, → "misfit dislocations"

→ semi-coherent interface

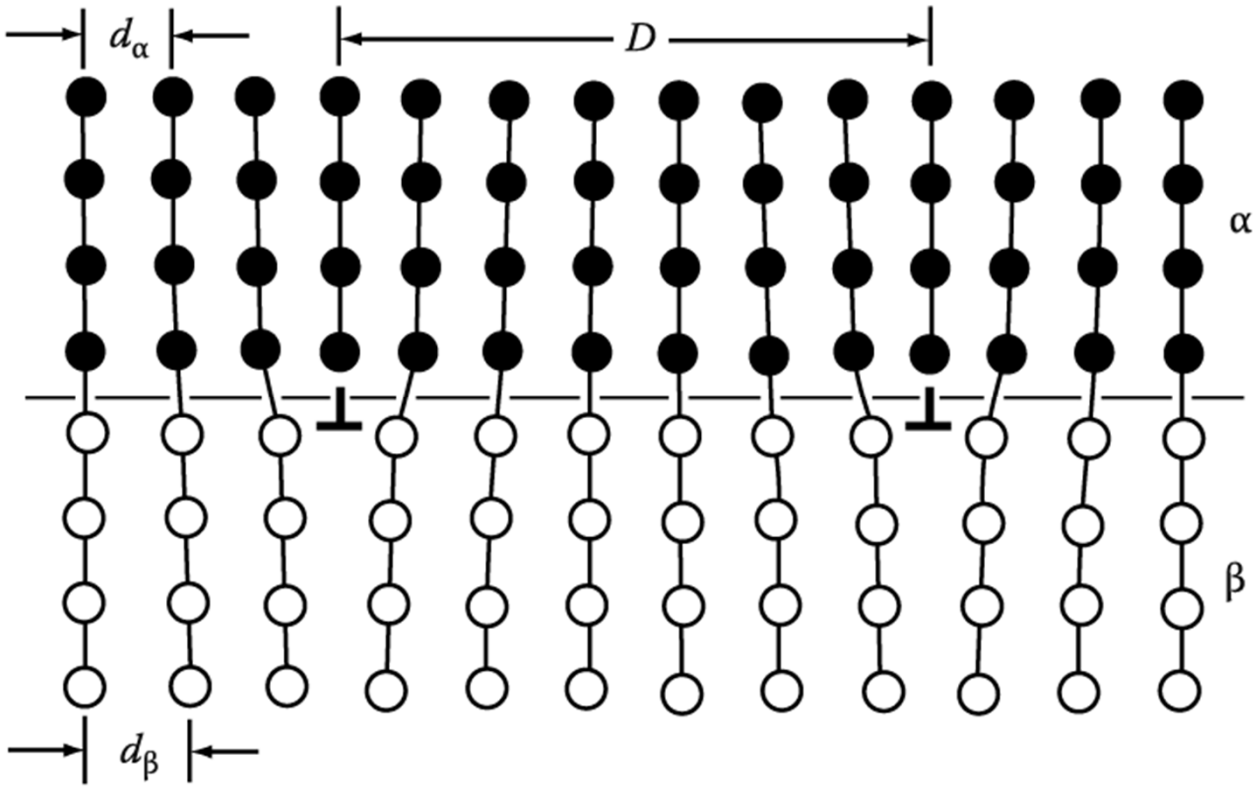

Misfit between the two lattices

$$\delta = \frac{d_\beta - d_\alpha}{d_\alpha}$$

δ~ small,

$$D = \frac{b}{\delta}$$

δ: misfit (disregistry)

b: Burgers vector of disl.

[$b=(d_\alpha + d_\beta)/2$]

Fig. 3.35 A semi-coherent interface. The misfit parallel to the interface is accommodated by a series of edge dislocations.

(2) Semicoherent interfaces

$d_\alpha < d_\beta$

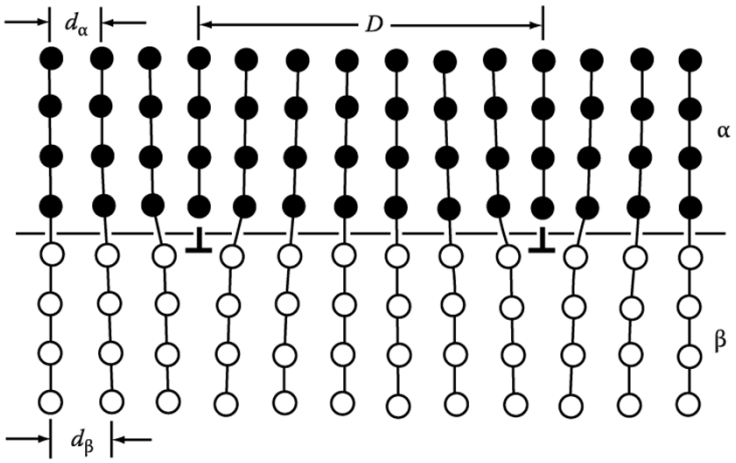

$\delta = (d_\beta - d_\alpha)/ d_\alpha$: misfit

→ D vs. δ vs. n

$(n+1)\, d_\alpha = n\, d_\beta = D$

$\delta = (d_\beta/ d_\alpha) - 1, (d_\beta/ d_\alpha) = 1 + 1/n = 1 + \delta$

→ $\delta = 1/n$

$D = d_\beta / \delta \approx b / \delta \quad [b=(d_\alpha + d_\beta)/2]$

δ~ small, Burgers vector of dislocation

$$\gamma(semicoherent) = \gamma_{ch} + \gamma_{st}$$

γ_{st} → due to **structural distortions** caused by the misfit dislocations

$$\gamma_{st} \propto \delta \text{ for small } \delta$$

In general,
γ (semicoherent) ~ 200~500 mJm^{-2}

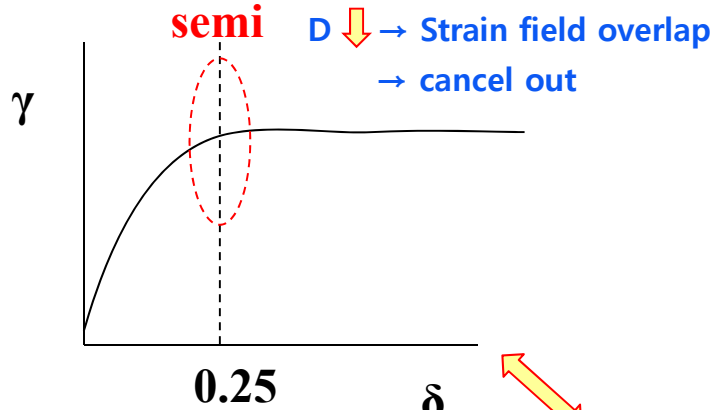

1 dislocation per 4 lattices
n=4

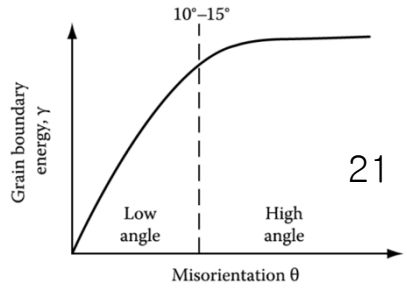

3) Incoherent Interfaces ~ high angle grain boudnary

1) δ > 0.25 No possibility of good matching across the interface

2) different crystal structure (in general)

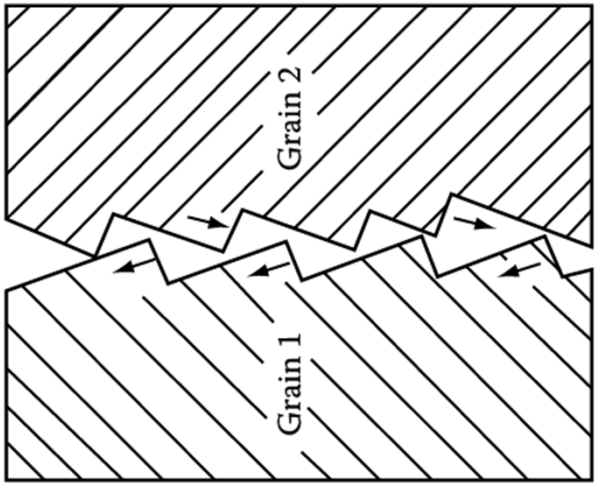

In general,
γ (incoherent) ~ 500~1000 mJm^{-2}

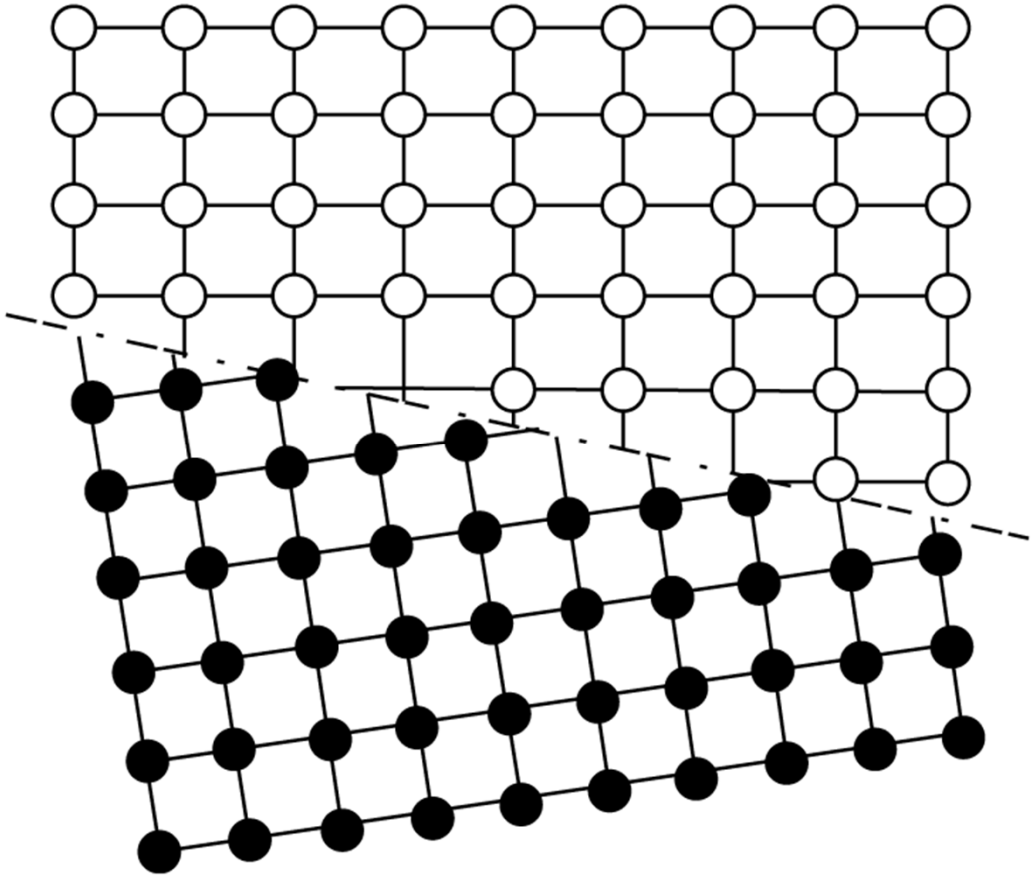

incoherent

Fig. 3.37 An incoherent interface.

4) Complex Semicoherent Interfaces

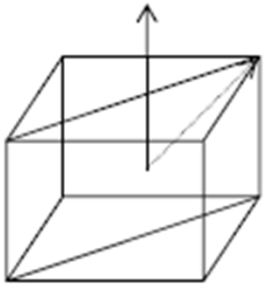

a_α=2.87

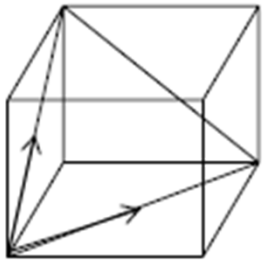

a_γ=3.57

If bcc α is precipitated from fcc γ, which interface is expected?

Which orientation would make the lowest interface energy?

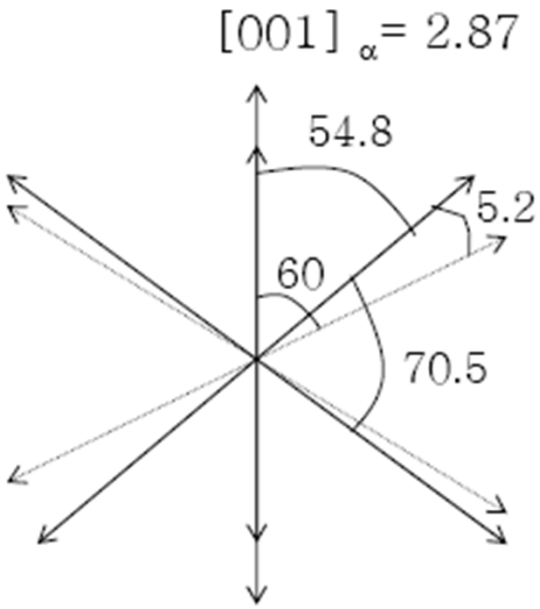

For fcc and bcc crystals ~ closest-pack planes in each phase almost parallel to each other

Nishiyama-Wasserman (N-W) Relationship

$$(110)_{bcc} // (111)_{fcc}, \quad [001]_{bcc} // [\bar{1}01]_{fcc}$$

Kurdjumov-Sachs (K-S) Relationships

$$(110)_{bcc} // (111)_{fcc}, \quad [1\bar{1}1]_{bcc} // [0\bar{1}1]_{fcc}$$

(The only difference between these two is a rotation in the closest-packed planes of 5.26°.)

Complex Semicoherent Interfaces

Semicoherent interface observed at boundaries formed by low-index planes.

(atom pattern and spacing are almost equal.)

N-W relationship

Good fit is restricted to small diamond-shaped areas that only contain ~8% of the orientation relationship.

A similar situation can be shown to exist for the K-S orientation relationship.

⇨ **But,**
impossible to form a large interfaces
→ Incoherent interface

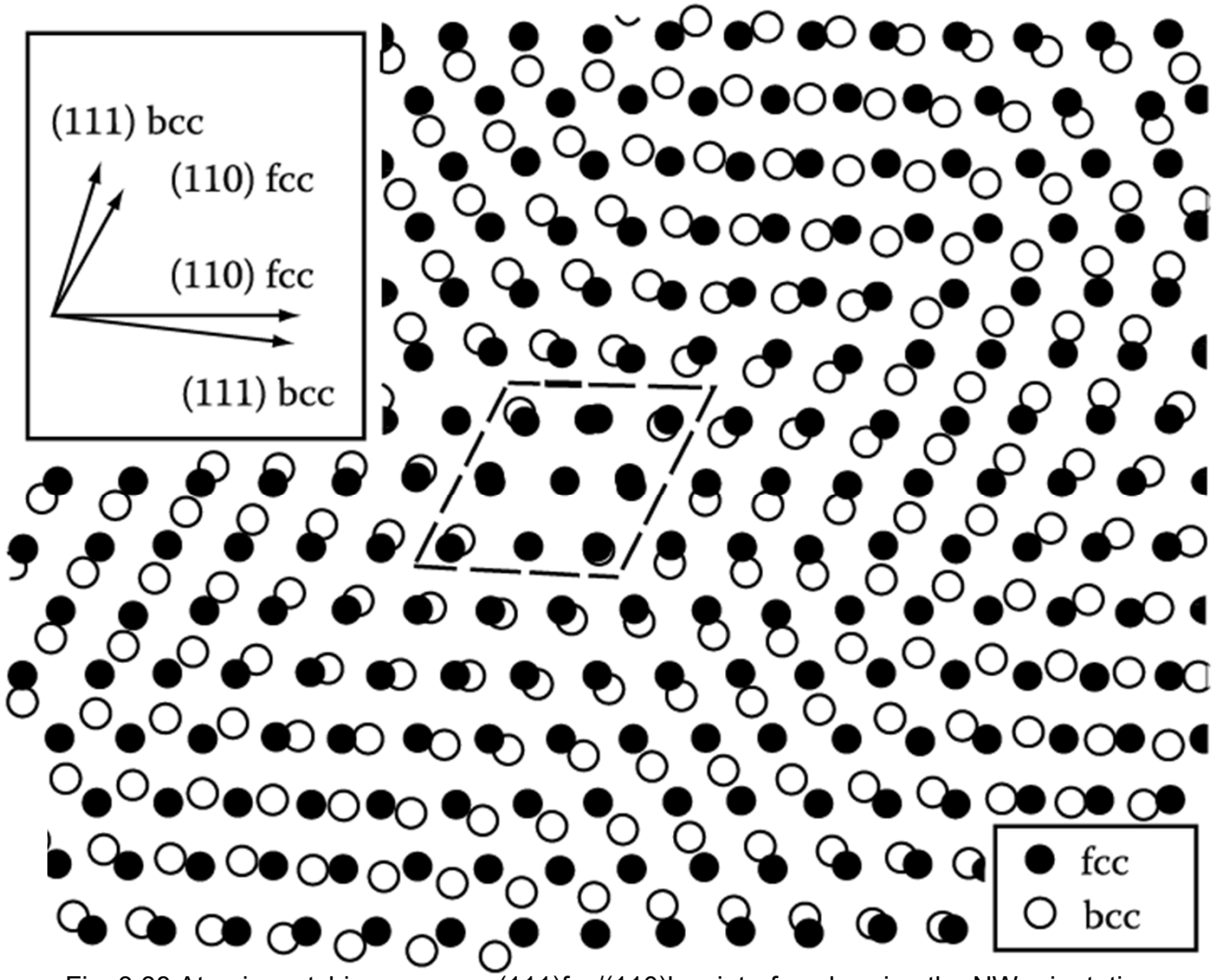

Fig. 3.38 Atomic matching across a (111)fcc/(110)bcc interface bearing the NW orientation relationship for lattice parameters closely corresponding to the case of fcc and bcc iron.

Complex Semicoherent Interfaces

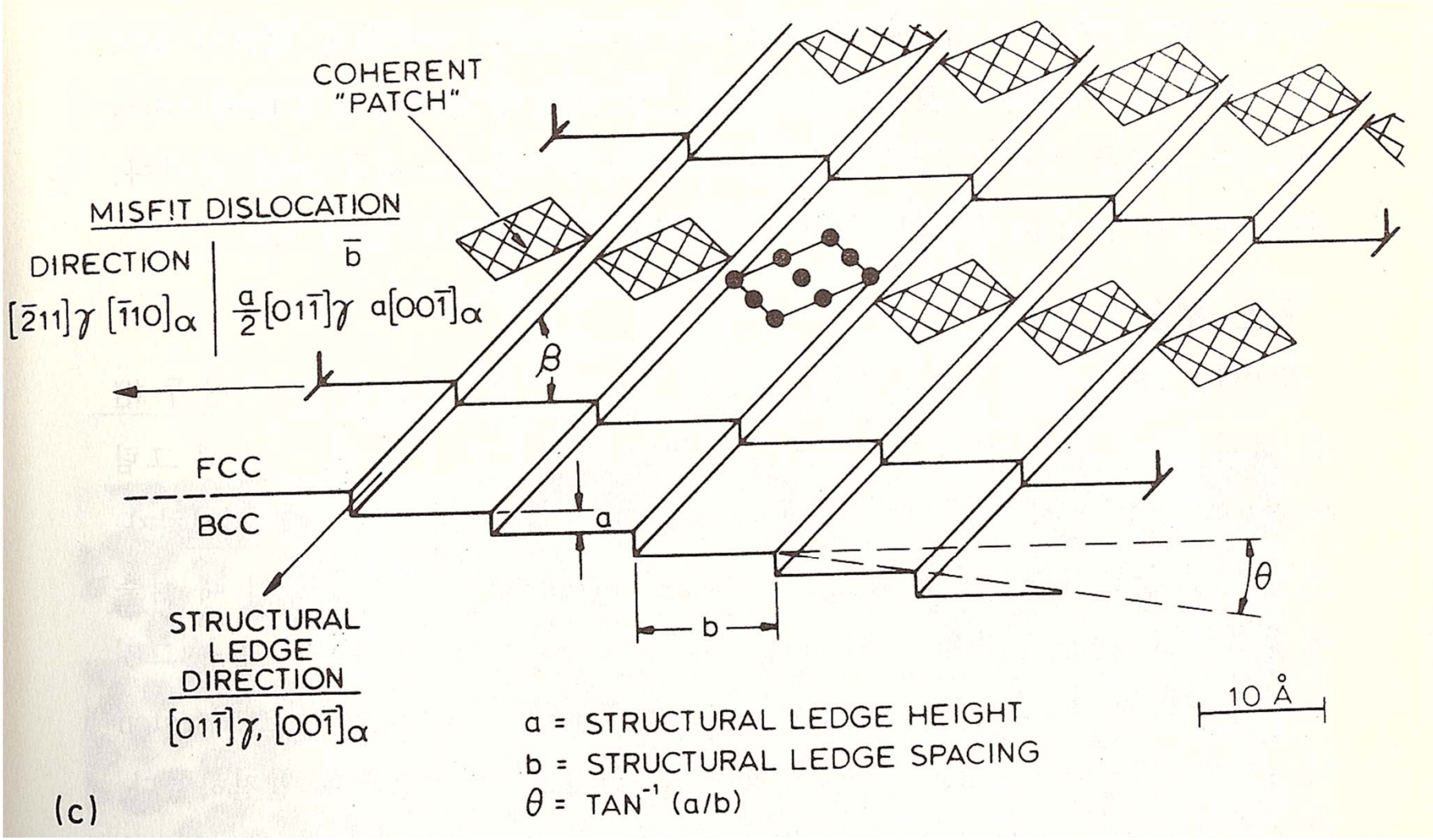

The degree of coherency can, however, be greatly increased if a macroscopically irrational interface is formed. The detailed structure of such interfaces is, however, uncertain due to their complex nature.

3.4 Interphase Interfaces in Solids

Interphase boundary - different two phases : different crystal structure
different composition

coherent, **Perfect atomic matching at interface**

γ **(coherent) =** γ_{ch} γ **(coherent) ~ 200 mJM^{-2}**

semicoherent $\gamma(semicoherent) = \gamma_{ch} + \gamma_{st}$

γ_{st} → due to structural distortions
caused by the misfit dislocations

γ**(semicoherent) ~ 200~500 mJM^{-2}**

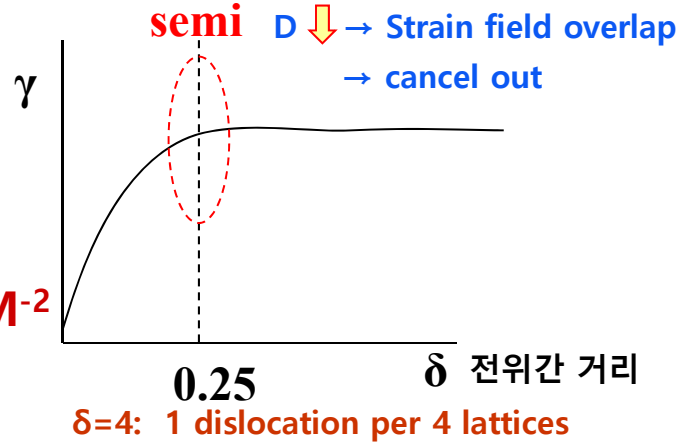

incoherent

1) δ > 0.25 No possibility of good matching across the interface

2) different crystal structure (in general)

γ **(incoherent) ~ 500~1000 mJM^{-2}**

Complex Semicoherent Interfaces

Nishiyama-Wasserman (N-W) Relationship **Kurdjumov-Sachs (K-S) Relationships**

(The only difference between these two is a rotation in the closest-packed planes of 5.26°.)

The degree of coherency can, however, be greatly increased if a macroscopically irrational interface is formed.

Q: How is the second-phase shape determined?

If misfit is small,
Equilibrium shape of a coherent precipitate or zone **can only be predicted from the "γ-plot"**

$$\sum A_i \gamma_i$$

⇨ Misfit

$$\sum A_i \gamma_i + \Delta G_S = minimum$$

"γ-plot" + "Elastic strain energy"

Lowest total interfacial free energy
by optimizing the shape of the precipitate and its orientation relationship

Fully coherent precipitates

γ_{ch} ⇨ γ_{ch} + *Lattice misfit* ⇨ γ_{ch} + $Volume\ Misfit\ \ \Delta = \frac{\Delta V}{V}$

different composition — Coherency strain energy — Chemical and structural interfacial E

Incoherent inclusions

(a) Precipitate shapes : $\sum A_i \gamma_i$ ⇩

(b) Calculation of misfit strain energy

3.4.2 Second-Phase Shape: Interfacial Energy Effects

How is the second-phase shape determined? $\sum A_i \gamma_i = minimum$

Lowest total interfacial free energy
by optimizing the shape of the precipitate and its orientation relationship

A. Fully Coherent Precipitates (G.P. Zone)

- If α, β have the same structure & a similar lattice parameter
- Happens during early stage of <u>many precipitation hardening</u>
- Good match ⇨ can have any shape ⇨ spherical

A zone with no misfit

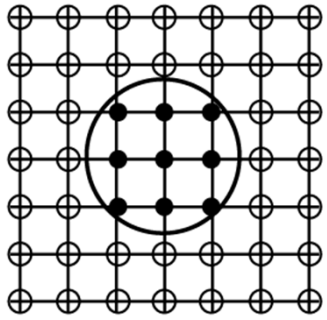

(a)

GP(Guinier- Preston) Zone in Al – Ag Alloys

$$\varepsilon_a = \frac{r_A - r_B}{r_A} = 0.7\%$$

→ **negligible contribution to the total free energy**

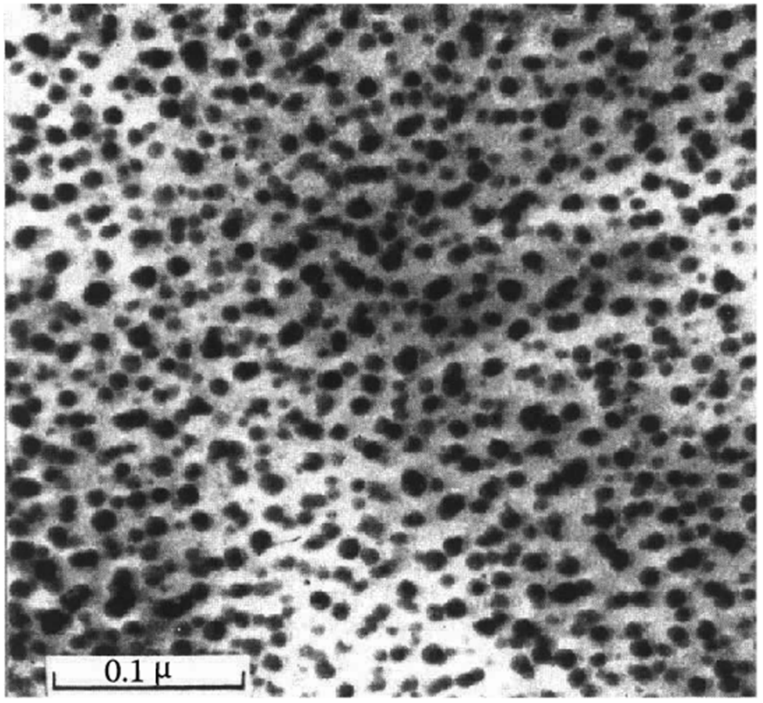

(b) Ag-rich GP zones (Dia. ~10 nm) in Al-4at% Ag alloy

B. Partially Coherent Precipitates

- α, β have different structure and one plane which provide close match

- **Coherent or Semi-coherent in one Plane;**
  Disc Shape (also plate, lath, needle-like shapes are possible)

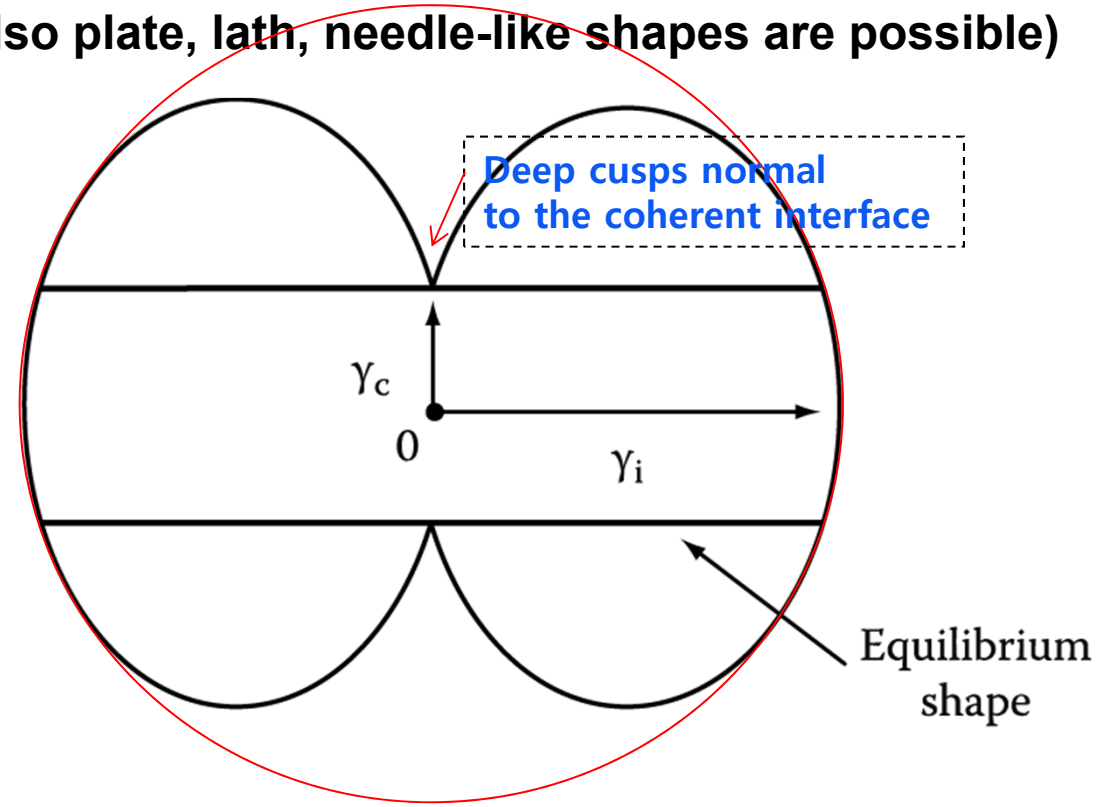

Fig. 3.40 A section through a **γ-plot** for a precipitate showing one coherent or semi-coherent interface, together with the equilibrium shape (a disc).

Precipitate shapes observed in practice
~ not equilibrium shape through a γ-plot
why? 1) misfit strain E effects ~ ignored.
2) different growth rates depending on directions

hcp γ′ Precipitates in Al – 4%Ag Alloys → plate

Semicoherent broad face parallel to the $\{111\}_\alpha$ matrix planes

(usual hcp/fcc orientation relationship)

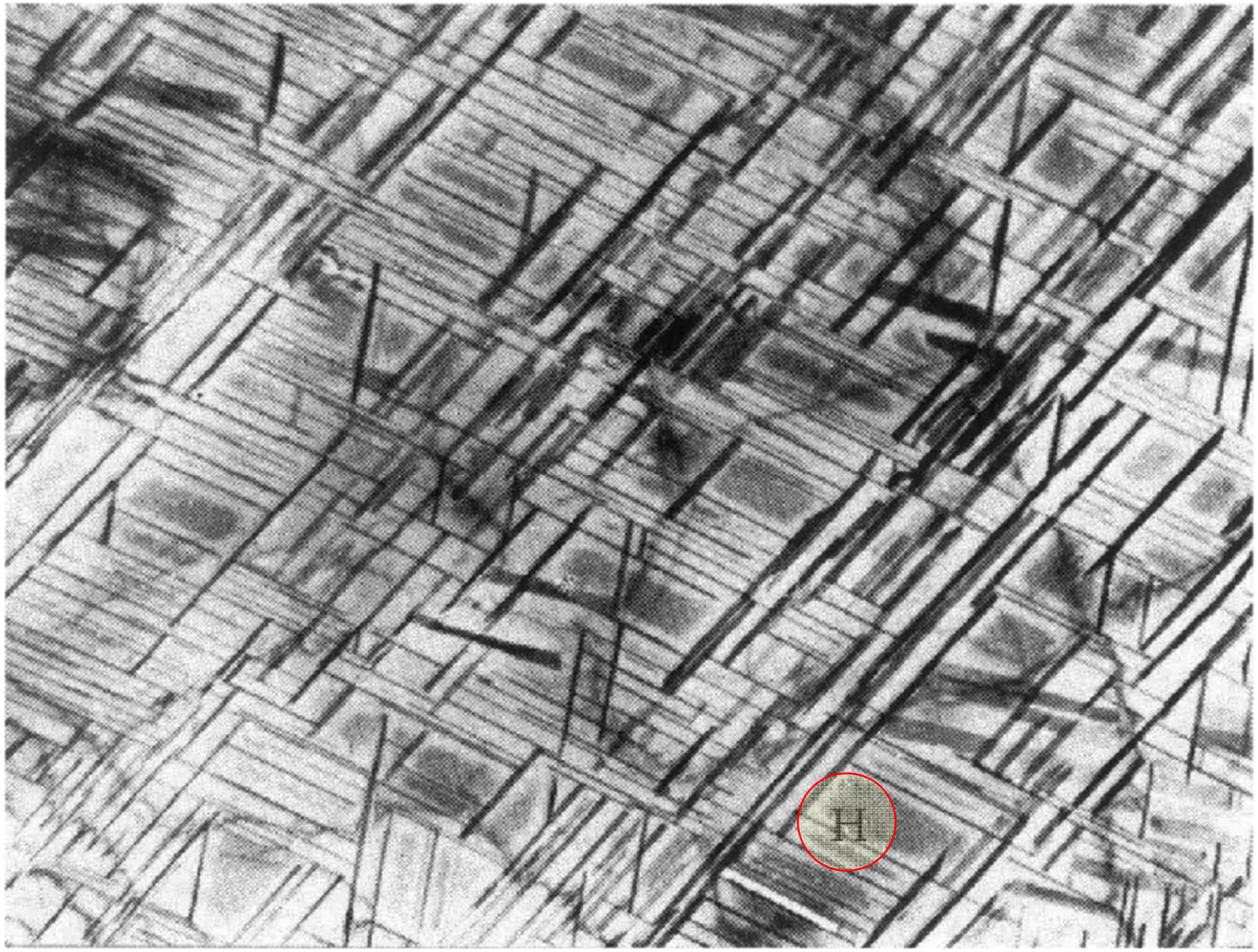

Fig. 3. 42 Electron micrograph showing the Widmanstatten morphology of γ' precipitates in an Al-4 atomic % Ag alloy. GP zones can be seen between the γ' e.g. at H (x 7000).

C. Incoherent precipitates

- when α, β have completely different structure ⇨ Incoherent interfaces
  or When the two lattices are in a random orientation
- Interface energy is high for all plane ⇨ spherical shape
  with smoothly curved interface
- Polyhedral shapes: certain crystallographic planes of the inclusion lie at cusps in the γ-plot

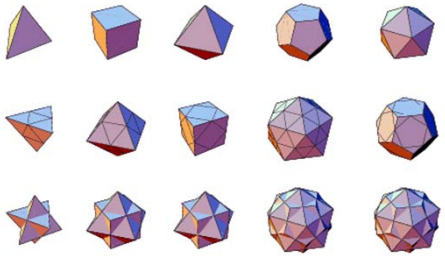

θ phase in $Al-Cu$ alloys (Al_2Cu)

Q: Example of Second-Phase Shape

precipitates from solid solution in Al-Cu alloys

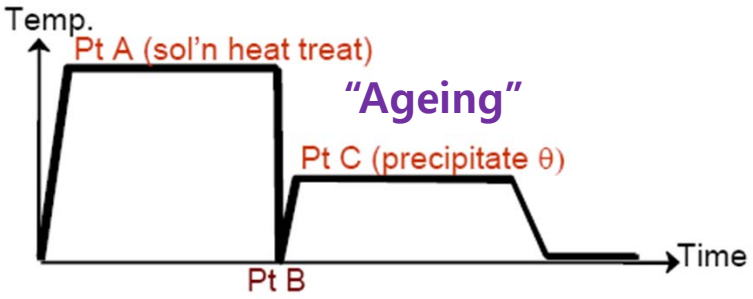

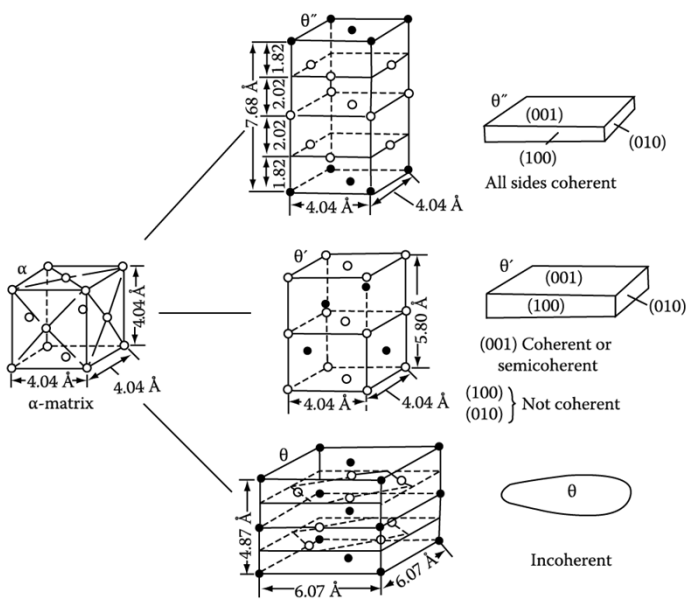

G.P. Zone

↓

θ", all coherent

↓

θ', partially coherent

↓

θ, incoherent

Precipitation Hardening

- Ex: Al-Cu system
- Procedure:

- *Pt A: solution heat treat (get a solid solution)*
- *Pt B: quench to room temp.*
- *Pt C: reheat to nucleate small θ crystals within α crystals.*

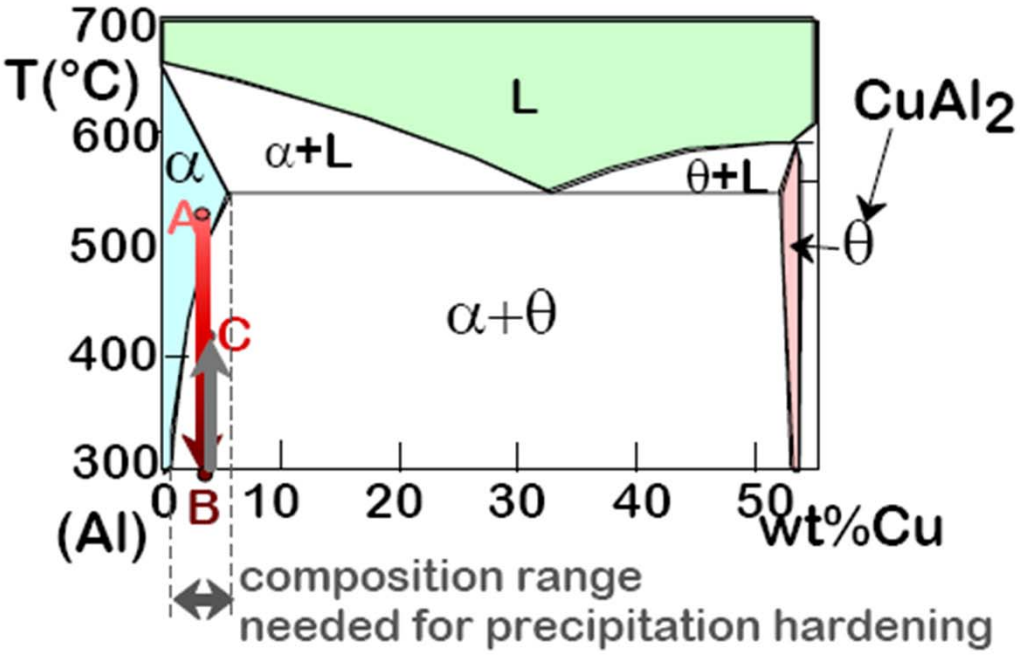

$\alpha + \theta \rightarrow$ Heat (~550°C) $\rightarrow$ Quench (0°C) $\rightarrow \alpha$ (ssss) $\rightarrow$ Heat/age (~150°C) $\alpha + \theta_{ppt}$

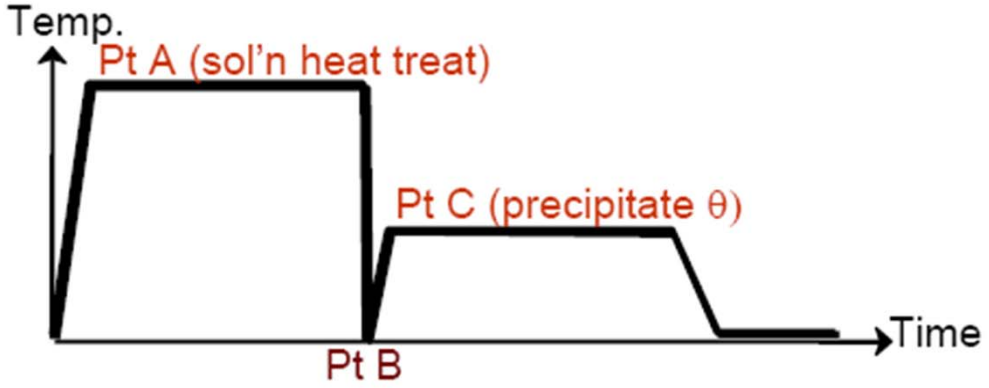

Al-Cu ppt structures

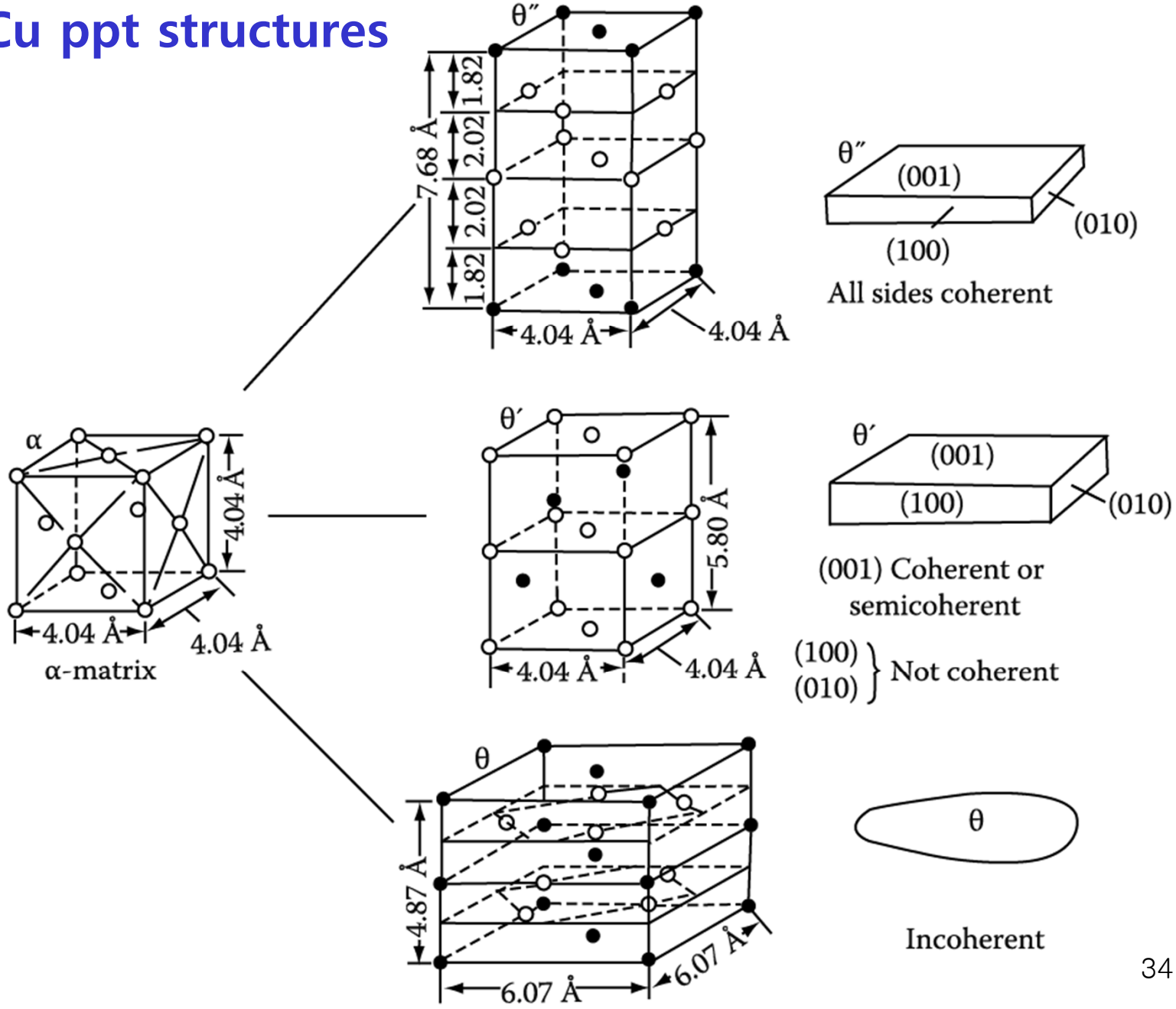

Al-Cu ppt structures

GP zone structure

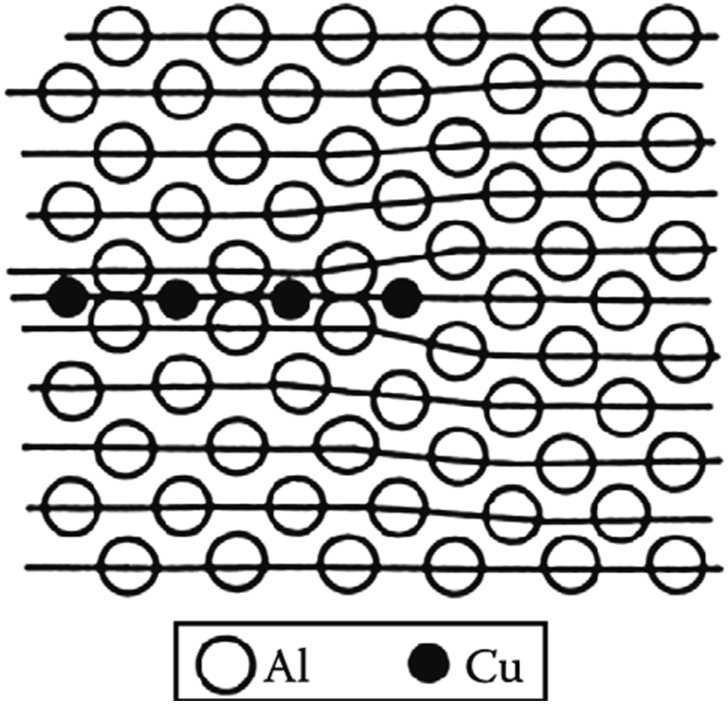

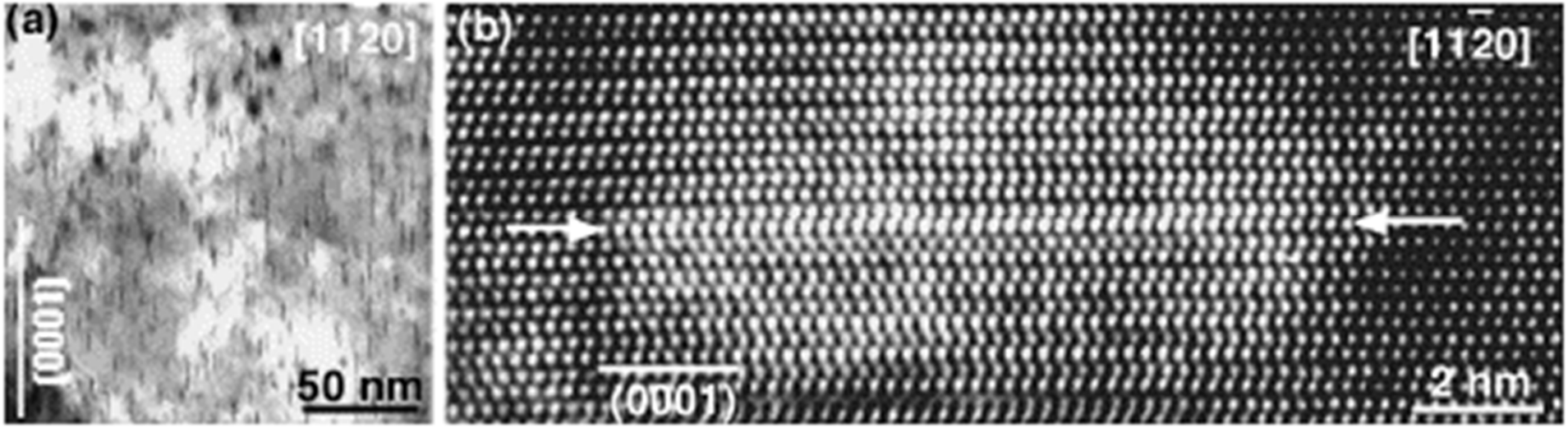

(a) Bright-field TEM image showing G.P. zones, and (b) HRTEM image of a G.P. zone formed on a single $(0\ 0\ 0\ 1)_\alpha$ plane. Electron beam is parallel to in both (a) and (b).

θ' Phase $Al-Cu$ Alloys

Semicoherent broad face parallel to the $\{100\}_\alpha$ matrix planes (habit plane)

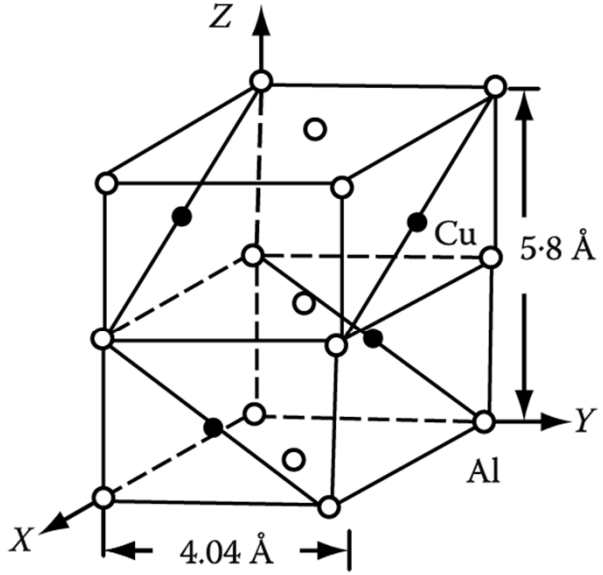

(a) The unit cell of the Θ′ precipitate in Al-Cu alloys

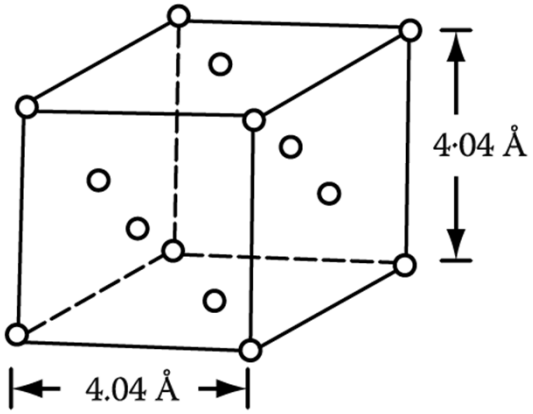

(b) The unit cell of the matrix

Orientation relationship between α and θ'

$$(001)_{\theta'} \;//\; (001)_{\alpha} \qquad [100]_{\theta'} \;//\; [100]_{\alpha}$$

→ Cubic symmetry of the Al-rich matrix (α) ~ many possible orientations for the precipitate plates within any given grain

S phase in Al-Cu-Mg alloys ; Lath shape

β' phase in Al-Mg-Si alloys ; Needle shape

} **Widmanstätten morphology**

θ phase in $Al-Cu$ alloys (Al_2Cu)

- **Polyhedral shapes:** certain crystallographic planes of the inclusion lie at cusps in the γ-plot

5.5.4. Age Hardening

Transition phase precipitation → great improvement in the mechanical properties
Coherent precipitates → highly strained matrix → dislocations~forced during deformation

Hardness vs. Time by Ageing

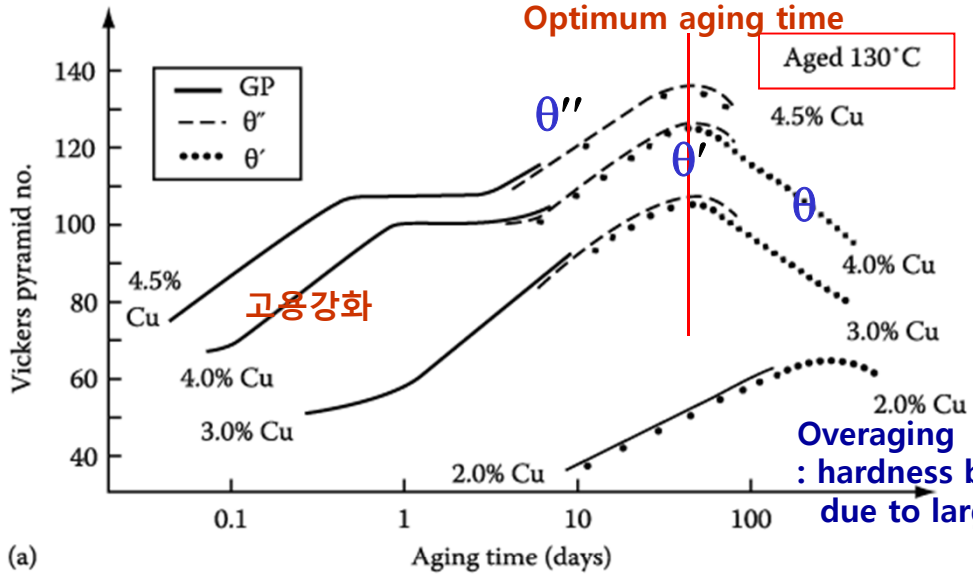

Maximum hardness~ largest fraction of θ″ (coherent precipitates)

Ageing at 130°C produces higher maximum hardness than ageing at 190°C.

At 130°C, however, it takes too a long time.

Overaging
: hardness begins to decrease due to large spacing between precipitates

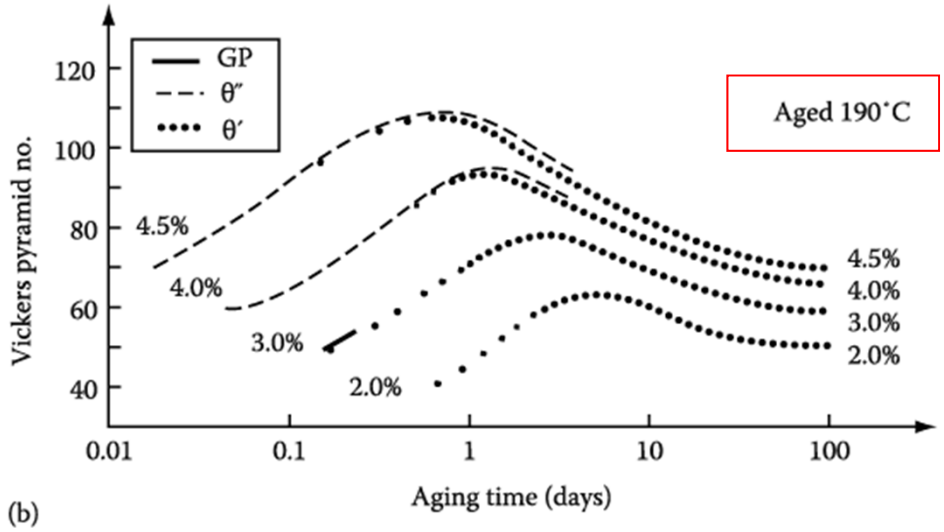

How can you get the high hardness for the relatively short ageing time?

Double ageing treatment
first below the GP zone solvus → fine dispersion of GP zones then ageing at higher T.

Finer precipitate distribution

Fig. 5. 37 Hardness vs. time for various Al-Cu alloys at (a) 130 ℃ (b) 190 ℃

Precipitates on Grain Boundaries

Formation of a second-phase particle at the interfaces with two differently oriented grains

1) incoherent interfaces with both grains

2) a coherent or semi-coherent interface with one grain and an incoherent interface with the other,

3) coherent or semi-coherent interface with both grains

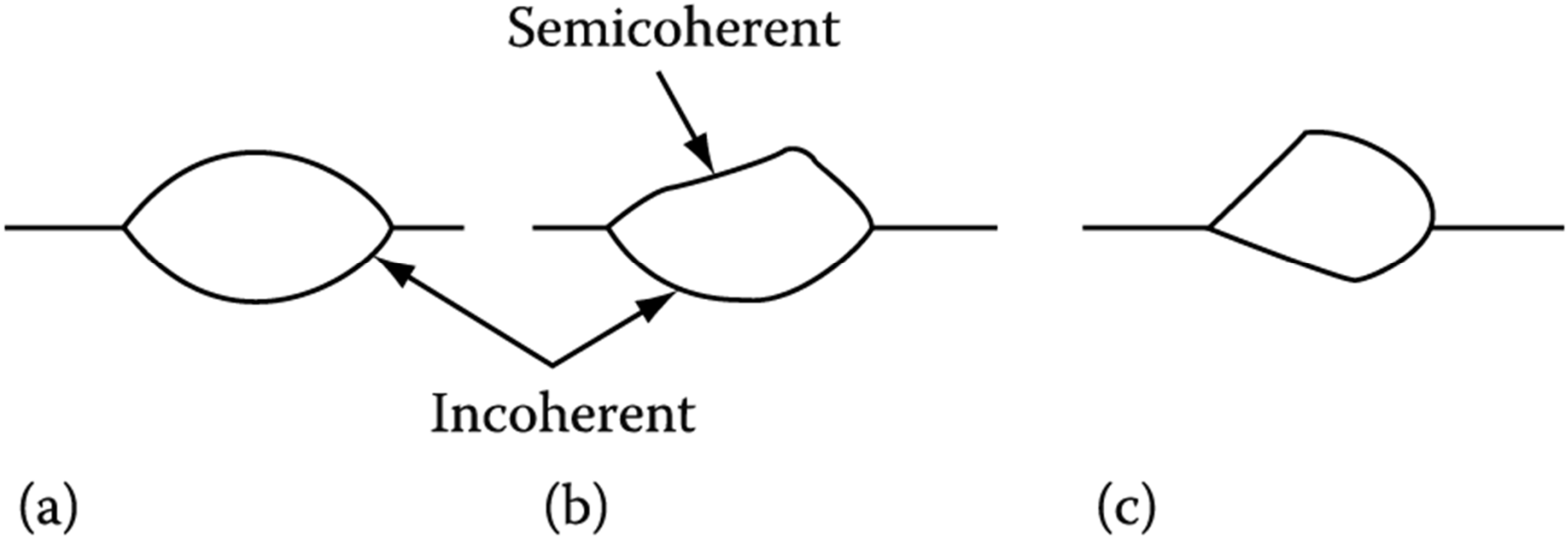

Fig. 3. 45 Possible morphologies for grain boundary precipitates. Incoherent interfaces smoothly curved. Coherent or semicoherent interface plannar.

Precipitates on Grain Boundaries

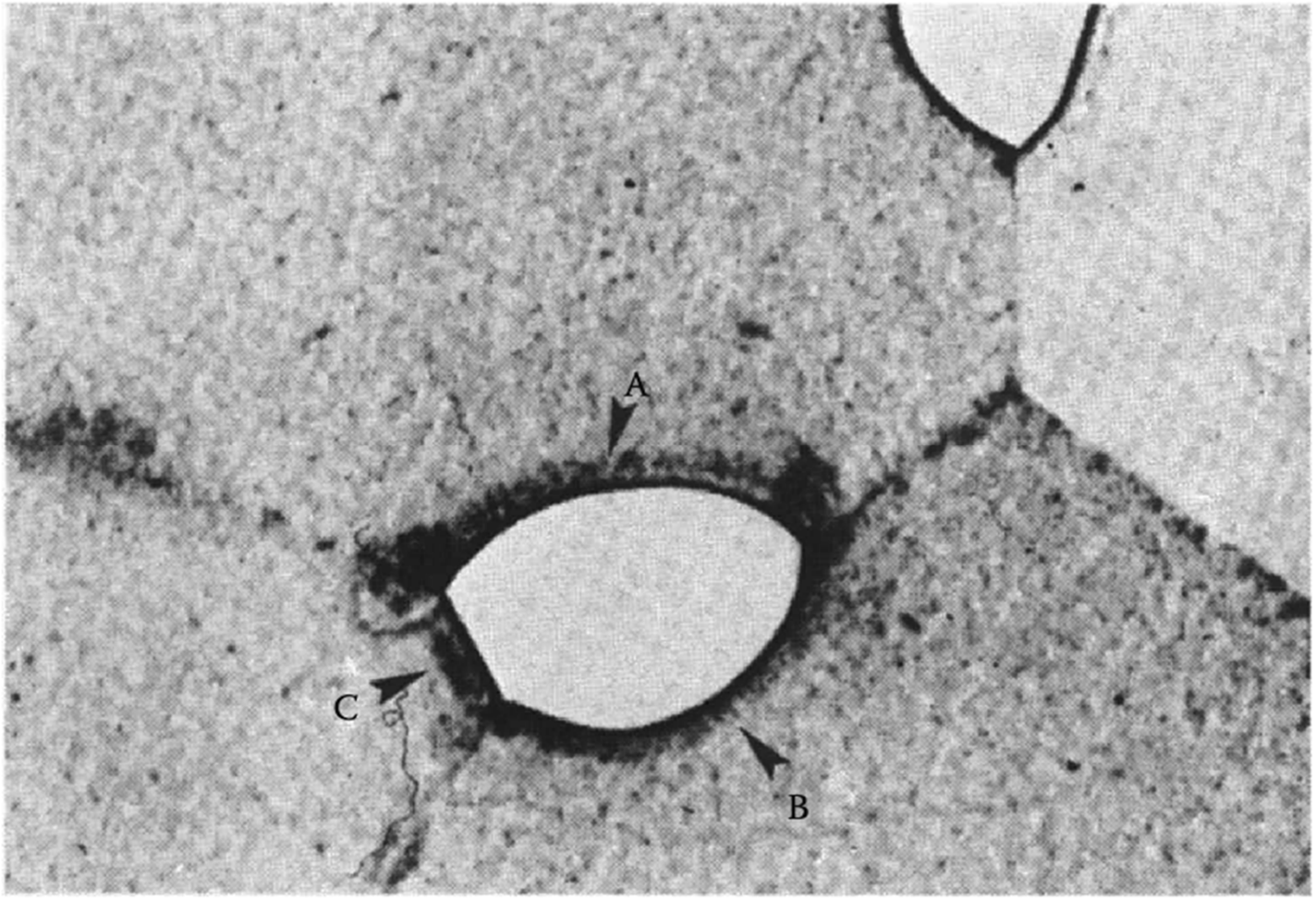

Fig. 3. 46 An α precipitate at a grain boundary triple point in an α – β Cu-In alloy. Interfaces A and B are incoherent while C is semicoherent (x 310).

A, B; Incoherent, C; Semi-coherent or coherent

3.4 Interphase Interfaces in Solids (α/β)

$$\sum A_i \gamma_i + \Delta G_S = minimum$$

1) Interphase boundary - different two phases : different crystal structure
different composition

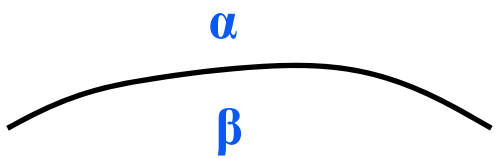

- Coherent/ Semicoherent/ Incoherent
- Complex Semicoherent

Fully coherent precipitates

γ_{ch} ⇨ γ_{ch} + *Lattice misfit* ⇨ γ_{ch} + $Volume\ Misfit\ \ \Delta = \frac{\Delta V}{V}$

different composition — Coherency strain energy — Chemical and structural interfacial E

Incoherent inclusions

2) Second-Phase Shape: precipitate from solid solution in Al-Cu alloys

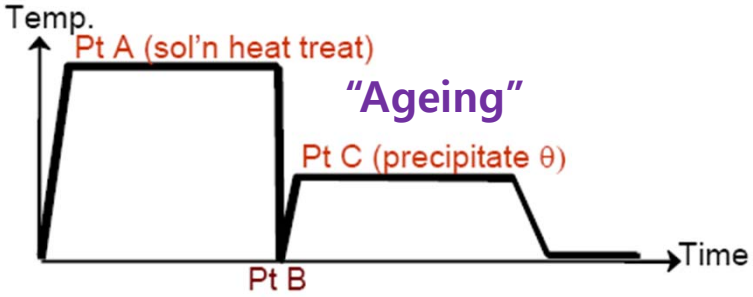

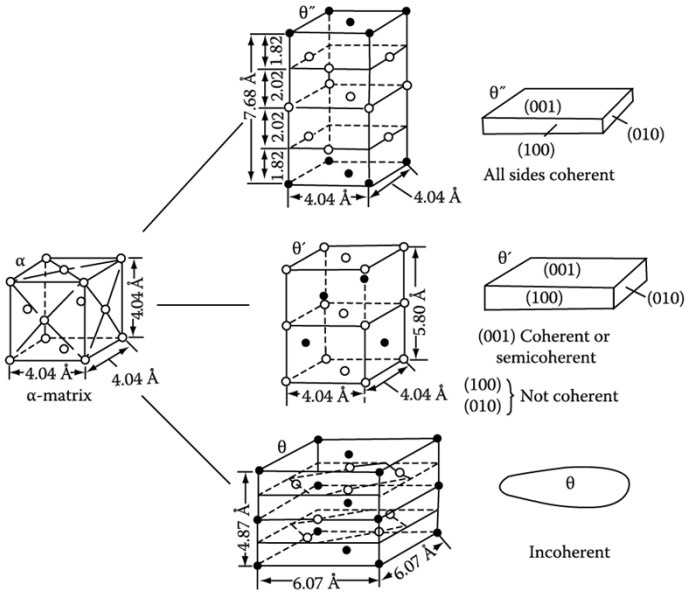

- **G.P. Zone**
- ⇩
- **θ", all coherent**
- ⇩
- **θ', partially coherent**
- ⇩
- **θ, incoherent**

Q: How is the second-phase shape determined?

$$\sum A_i \gamma_i + \Delta G_S = minimum$$

γ – plot + misfit strain E

Lowest total interfacial free energy
by optimizing the shape of the precipitate and its orientation relationship

Fully coherent precipitates

γ_{ch} ⇨ γ_{ch} + *Lattice misfit* ⇨ γ_{ch} + $Volume\ Misfit\quad \Delta = \frac{\Delta V}{V}$

different composition — Coherency strain energy — Chemical and structural interfacial E

Incoherent inclusions

(a) Precipitate shapes

(b) Calculation of misfit strain energy

3.4.3. Second-Phase Shape: Misfit Strain Effects

If misfit is small,
Equilibrium shape of a coherent precipitate or zone can only be predicted from the "γ-plot"

$\sum A_i \gamma_i$

Misfit ⇒ $\sum A_i \gamma_i + \Delta G_S = minimum$

"γ-plot" + "Elastic strain energy"

A. Fully Coherent Precipitates

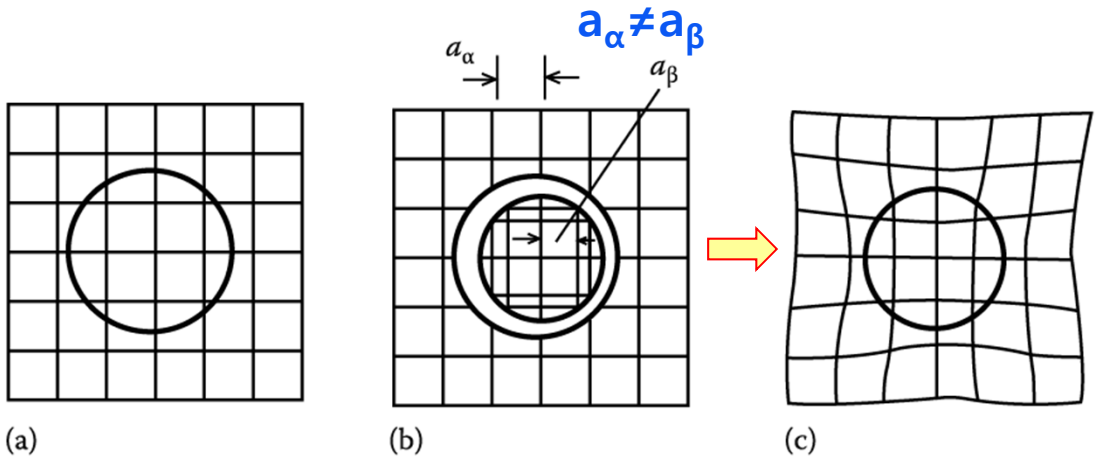

Distortion (격자변형) is pure hydrostatic, i.e., it is uniform in all directions. → new lattice parameter a_β'

Fig. 3. 47 The origin of coherency strains. The number of lattice points in the hole is conserved.

Unconstrained Misfit *Constrained Misfit*

구속되지 않은 불일치도 $\delta = \frac{a_\beta - a_\alpha}{a_\alpha}$ ⇒ 구속된 불일치도 $\varepsilon = \frac{a'_\beta - a_\alpha}{a_\alpha}$

① If $E_\beta = E_\alpha, \nu = 1/3 \rightarrow \varepsilon = \frac{2}{3}\delta$

Poisson's ratio

② In practice, different elastic constants $E_\beta \neq E_\alpha \rightarrow 0.5\delta \leq \varepsilon \leq \delta$

if thin disc-type precipitate,

⇨ **In situ misfit is no longer equal in all directions**

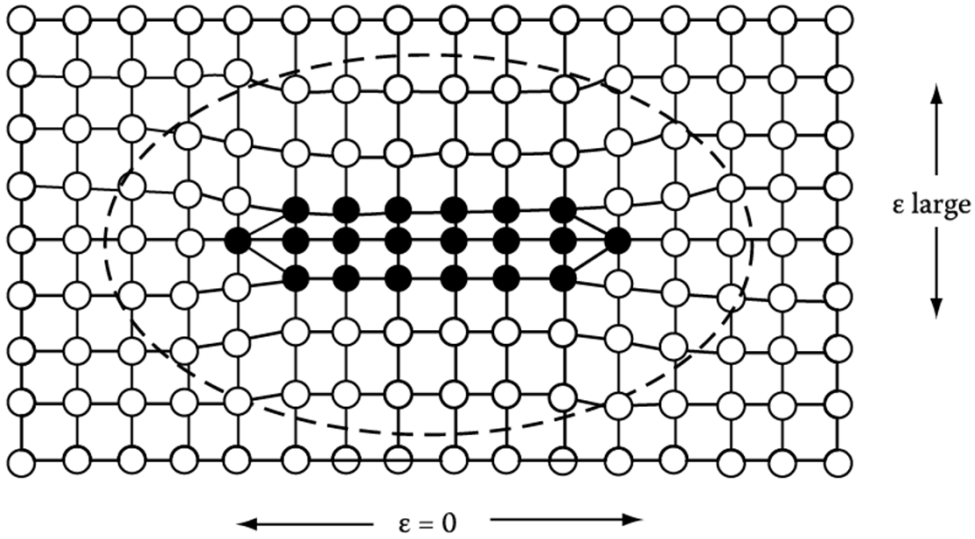

Fig. 3. 48 For a coherent thin disc there is **little misfit parallel to the plane of the disc. Maximum misfit is perpendicular to the disc. → reduction in coherency strain E**

* **Total elastic energy (ΔG_s) depends on the "shape" and "elastic properties" of both matrix and inclusion.**

Elastically Isotropic Materials & $E_\beta = E_\alpha$

$\Delta G_S = 4\mu\delta^2 \cdot V$ (If ν=1/3)

here, μ= shear modulus of the matrix,

V= volume of the unconstrained hole in the matrix

ΔG_S→ independent of the shape of the precipitate

Elastically Anisotropic Materials & $E_\beta \neq E_\alpha$

ΔG_S→ dependent of the shape of the precipitate

ΔG_S^{min}: if inclusion is hard→sphere/ soft→disc shape

Atom radius ($\overset{o}{A}$)	*Al* : 1.43	*Ag* : 1.44	*Zn* : 1.38	*Cu* : 1.28
Zone Misfit (δ)	–	+ 0.7 %	– 3.5 %	– 10.5 %
***GP** Zone Shape*	–	*sphere*	*sphere*	*disc*

Equilibrium shape

$\sum A_i\gamma_i + \Delta G_S = minimum$

Interfacial E effect dominant

$\delta < 5\%$

strain E effect dominant

Influence of strain E (δ =lattice misfit) on the equilibrium shape of coherent precipitation

B. Incoherent Inclusions

Lattice sites are not conserved. → no coherency strain, ΔG_S

But, misfit strain still arise if the inclusion is the wrong size.

δ (lattice misfit) → Δ (volume misfit)

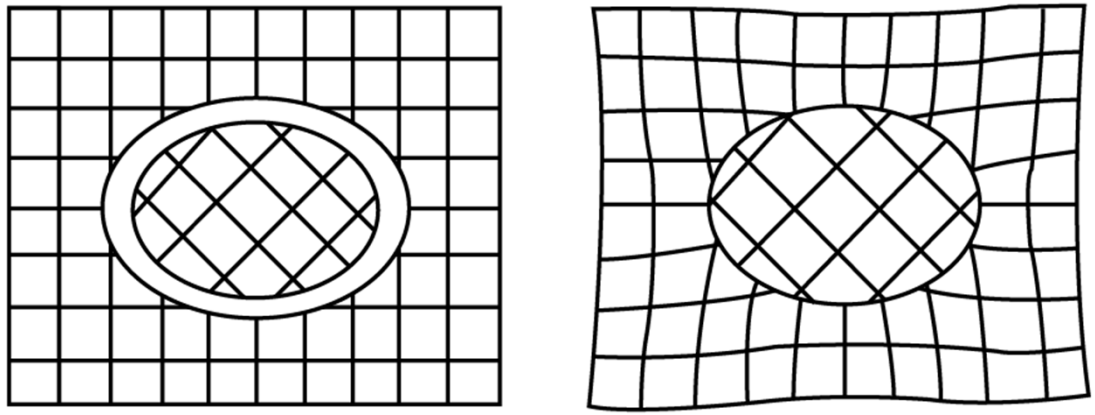

(a) (b)

#of lattice sites within the hole is not preserved for incoherent inclusion (no lattice matching)

$$\text{Volume Misfit} \quad \Delta = \frac{\Delta V}{V}$$

Ex) coherent spherical inclusion: $\Delta = 3\delta$

For spheroidal Inclusions $\dfrac{x^2}{a^2} + \dfrac{y^2}{b^2} + \dfrac{z^2}{c^2} = 1$

For Elliptical Inclusions $\dfrac{x^2}{a^2} + \dfrac{y^2}{a^2} + \dfrac{z^2}{c^2} = 1$

For a homogeneous incompressible inclusion in an isotropic matrix

등방성 기지내 균질 비압축성 개재물

Nabarro Eq.

$$\Delta G_S = \frac{2}{3}\mu\Delta^2 \cdot V \cdot f(c/a)$$

μ: the shear modulus of the matrix

1) The elastic strain energy is proportional to the square of the volume misfit Δ^2.

2) Shape effect for misfit strain E ~ function f (c/a)

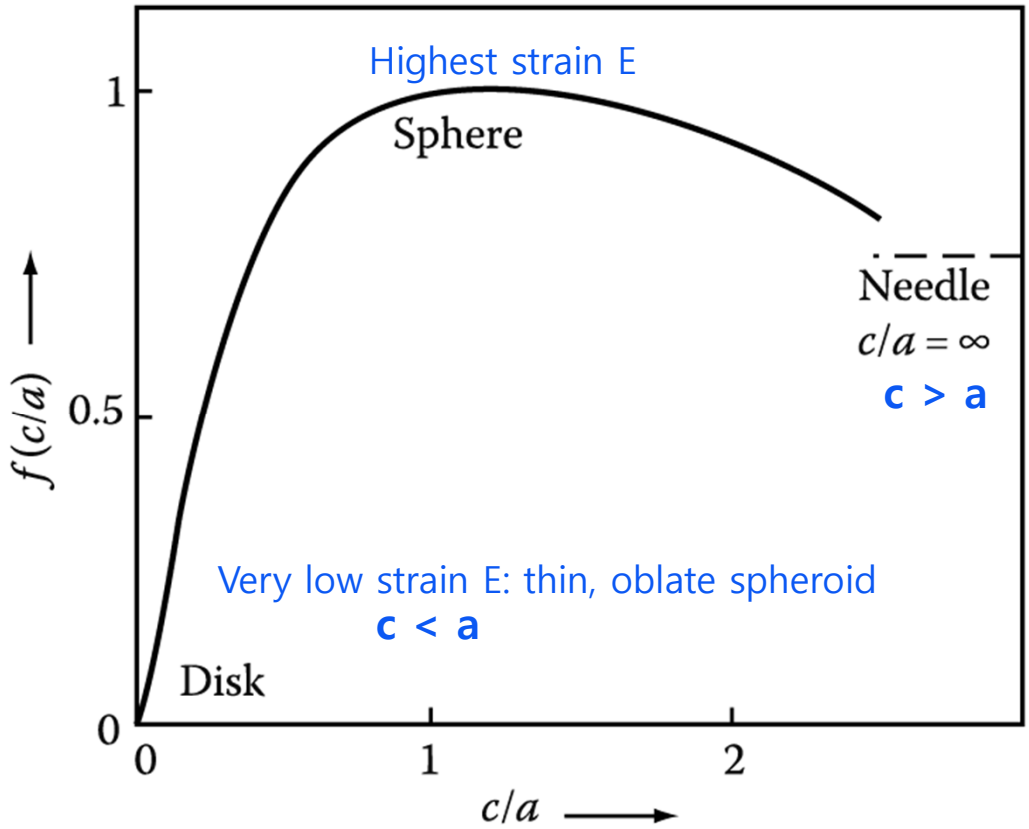

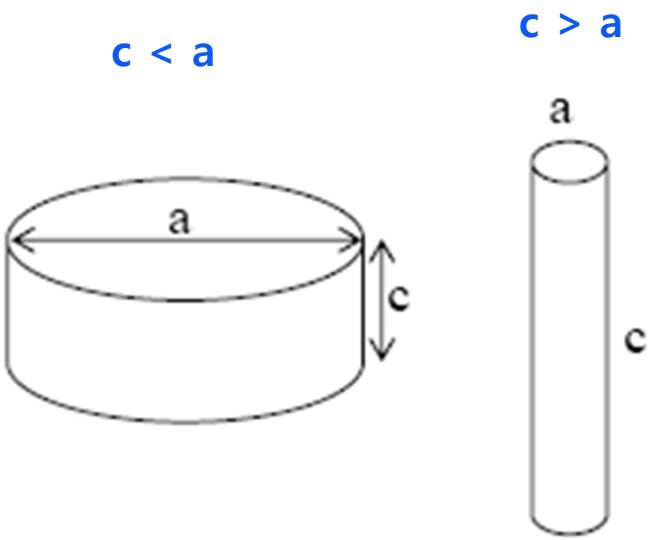

If elastic anisotropy is included, same general form for f(c/a) is preserved.

Fig. 3. 50 The variation of misfit strain energy with ellipsoid shape, f(c/a).

$$\Delta G_s = \frac{2}{3}\mu \Delta^2 \cdot V \cdot f(c/a) \qquad \Delta = \frac{V_\beta - V_\alpha}{V_\alpha} \approx 3\delta \text{ for sphere}, \neq 3\delta \text{ for disc or needle}$$

Elastic strain E

Precipitate shape effect

* Equil. Shape of an incoherent inclusion: an oblate spheroid with c/a value that balances the opposing effects of interfacial E and strain E

(here, $\Delta \sim$ small → Interfacial E dominant → roughly spherical inclusion)

C. Plate-like precipitates

Misfit across the broad faces → large coherency strains parallel to the plate

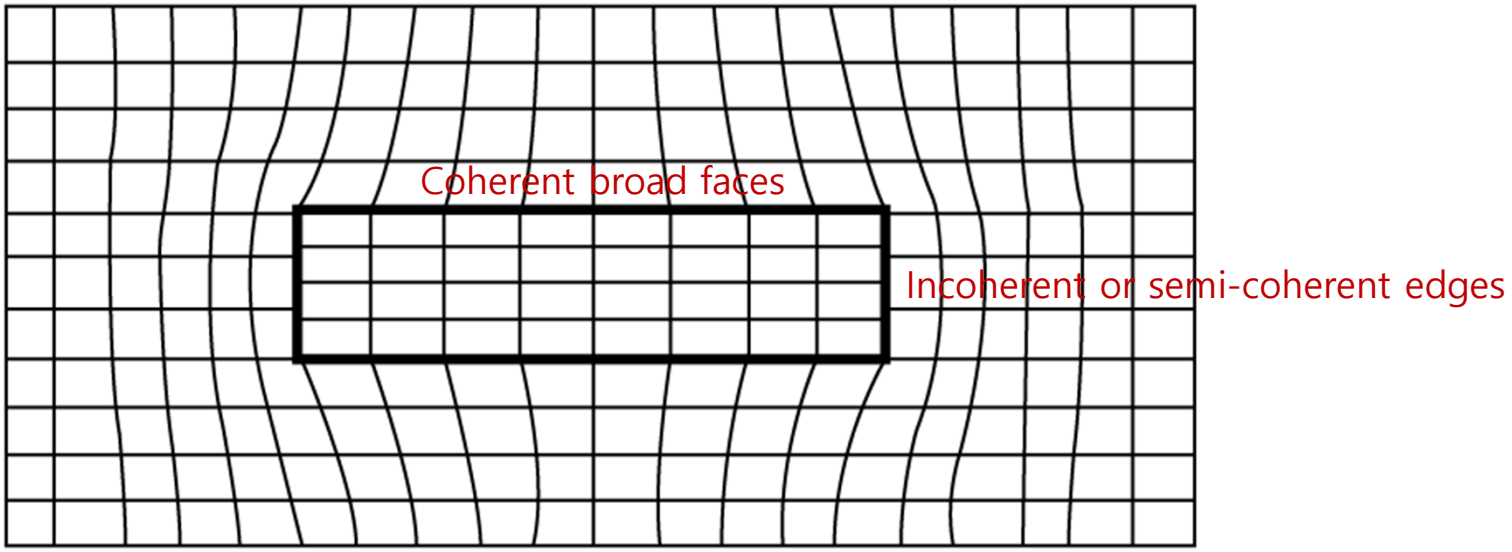

In situ misfit across the broad faces increases with increasing plate thickness

→ **greater strains the matrix and higher shear stresses at the corners of the plates**

→ **energetically favorable for the broad faces to become semi-coherent**

→ **the precipitate behaves as an incoherent inclusion with comparatively little misfit strain E, ex) θ' phase in Al-Cu alloy**

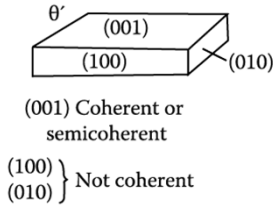

Q: Which state produces the lowest total E for a spherical precipitate?

"Coherency loss"

If a coherent precipitate grows, during aging for example, It should lose coherency when it exceeds r_{crit}.

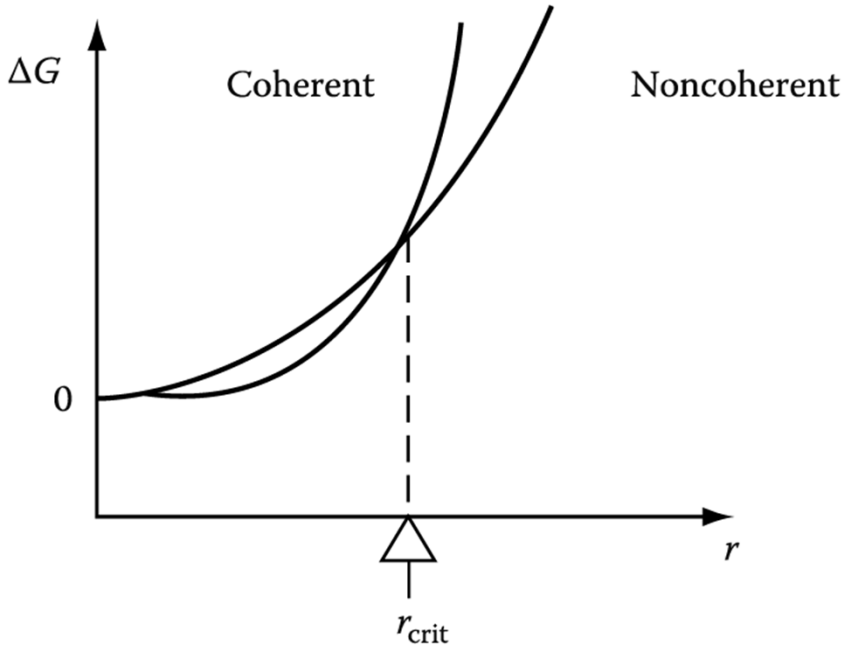

Coherency Loss

- Precipitates with coherent interfaces=low interfacial E + coherency strain E
- Precipitates with non-coherent interfaces=higher interfacial E

If a coherent precipitate grows, it should lose coherency to maintain minimum interfacial free E.

$$\Delta G(coherent) = 4\mu\delta^2 \cdot \frac{4}{3}\pi r^3 + 4\pi r^2 \cdot \gamma_{ch} \quad \Leftrightarrow \quad \Delta G(non-coherent) = 4\pi r^2 \cdot (\gamma_{ch} + \gamma_{st})$$

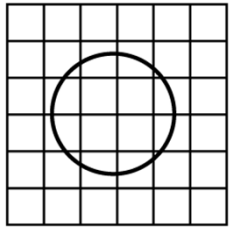

Coherency strain energy
Eq. 3.39

Chemical interfacial E

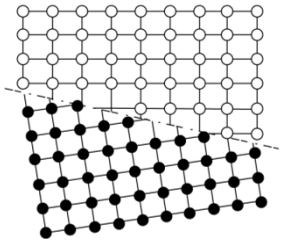

Chemical and structural interfacial E

$$\frac{4}{3}\pi r^3\left(4\pi\mu\delta^2\right) + 4\pi r^2\left(\gamma_{ch}\right) = 4\pi r^2\left(\gamma_{st} + \gamma_{ch}\right)$$

coherent ΔG_s-relaxed

$$\therefore r_{crit} = \frac{3\cdot\gamma_{st}}{4\mu\delta^2}$$

$$for\ small\ \delta,\quad \gamma_{st} \propto \delta$$

(semi-coherent interface)

$$\approx \frac{1}{\delta}$$ ($\delta = (d_\beta - d_\alpha)/ d_\alpha$: misfit)

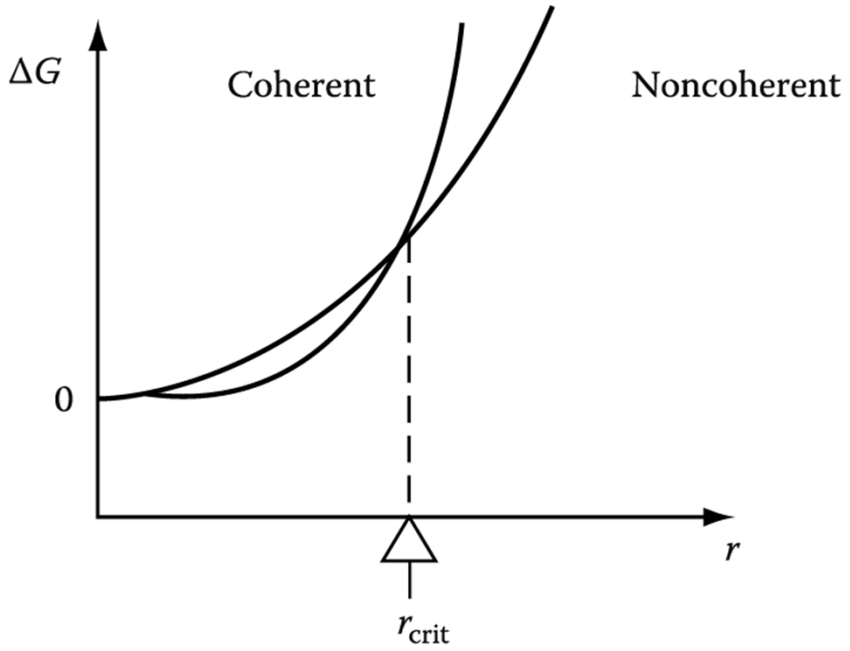

Fig. 3. 52 The total energy of matrix + precipitate vs. precipitate radius for spherical coherent and non-coherent (semicoherent of incoherent) precipitates.

If a coherent precipitate grows, during aging for example,
It should lose coherency when it exceeds r_{crit}.

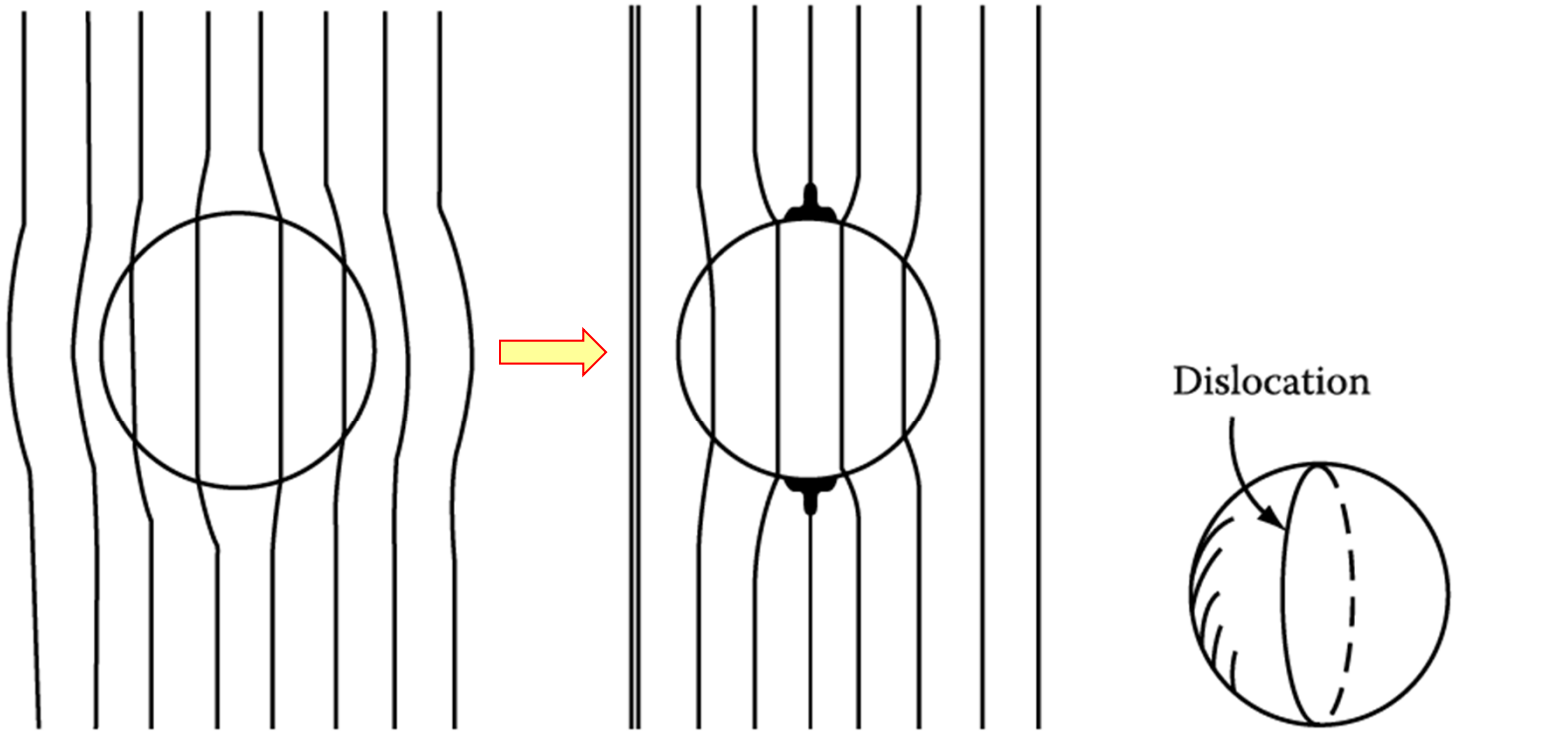

(a) Coherent with strain E (b) Coherency strain replace by dislocation loop. (c) Precipitate with dislocation

Fig. 3.53. Coherency loss for a spherical precipitate

In practice, this phenomena can be rather difficult to achieve.
→ Coherent precipitates are often found with sizes much larger than r_{crit}.

"Mechanisms for coherency loss": all require the precipitate to reach a larger size than r_{crit}

1) spherical precipitate

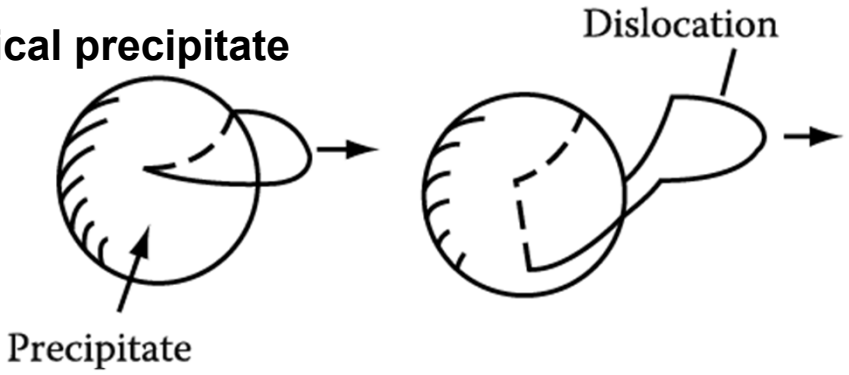

* Punching stress (P_s) ~ independent of size, but $P_s \propto$ constrained misfit, ε ($>\varepsilon_{crit}\sim0.05$), → "precipitates with a smaller ε cannot lose coherency by (a), no matter how large."

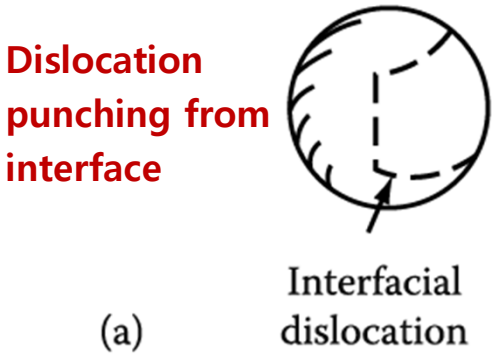

Dislocation punching from interface

requires the stresses at the interface to exceed the theoretical strength of the matrix

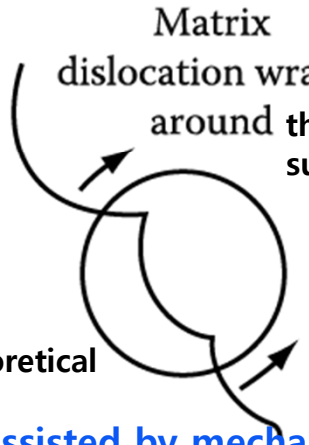

the precipitate with a suitable Burgers vector

assisted by mechanical deformation

(b) Capture of matrix dislocation

2) Plate precipitate

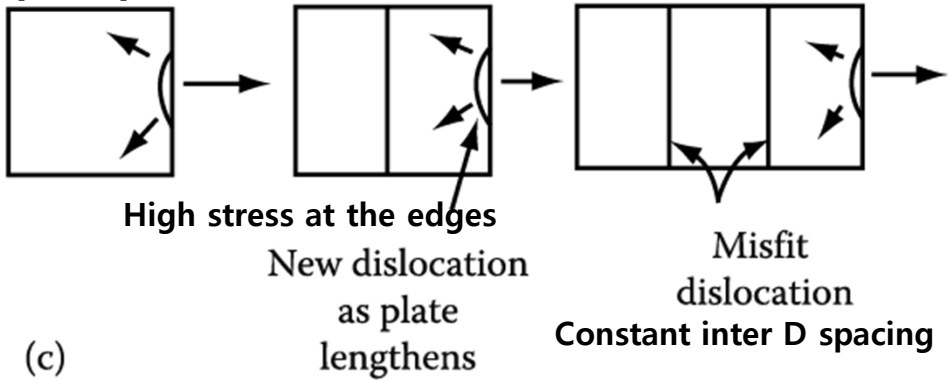

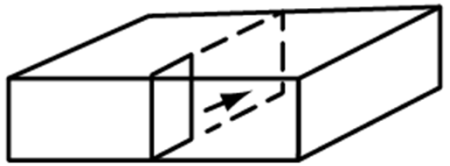

Prismatic dislocation loop

Nucleation of D loops within the precipitate

Nucleation of dislocation at the edge → maintain a roughly constant inter-dislocation spacing during plate lengthening

(d) Vacancies can be attracted to coherent interfaces and 'condense' to form a prismatic dislocation loop which can expand across the precipitate

Q: What is Glissile interface?

Glissile interface → coordinated glide of the interfacial disl. → (α→β) phase transformation

Interphase Interfaces in Solid (α/β)

1) Glissile Interfaces (평활 이동 계면)

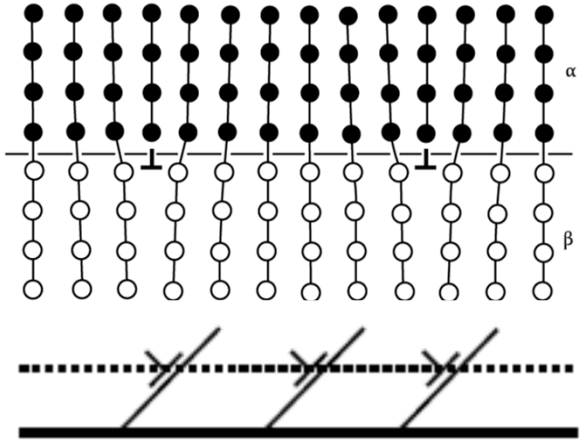

: epitaxial; Can't move forward or backward

(interface//burgers vector) ⟶ Non-glissile interface

: Glide of the interfacial disl. cannot cause the interface to advance

: Glissile; Boundary moves toward α or β

: semi-coherent interfaces which can advance by the coordinated glide of the interfacial disl.

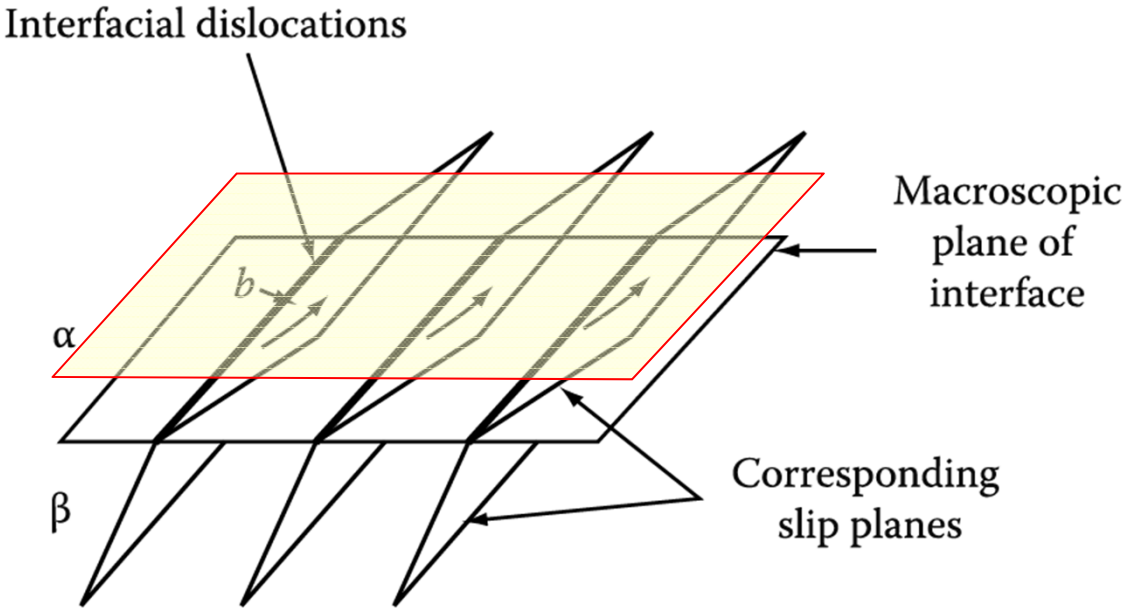

Fig. 3. 55 The nature of a glissile interface.

The dislocations have a Burgers vector that can glide on matching planes in the adjacent lattices.

Slip planes : continuous across the interface

Gliding of the dislocation :
α is sheared into the β structure.

Low-Angle tilt Boundaries

Bugers vector = edge dislocation

But, this is not interphase interface.

∵ crystal structure is same,
only lattice rotation

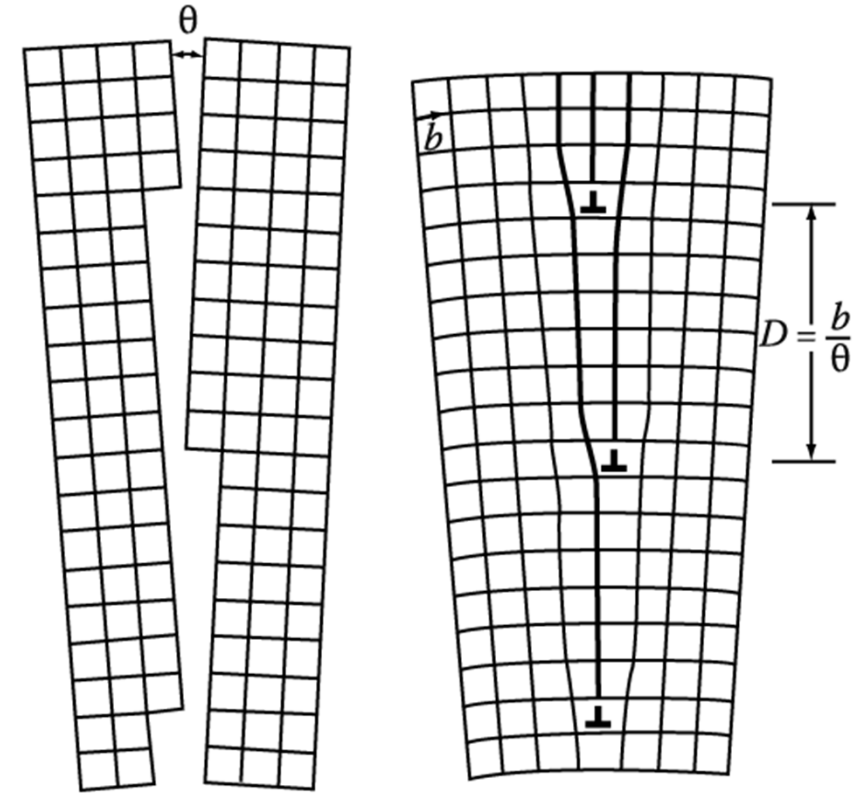

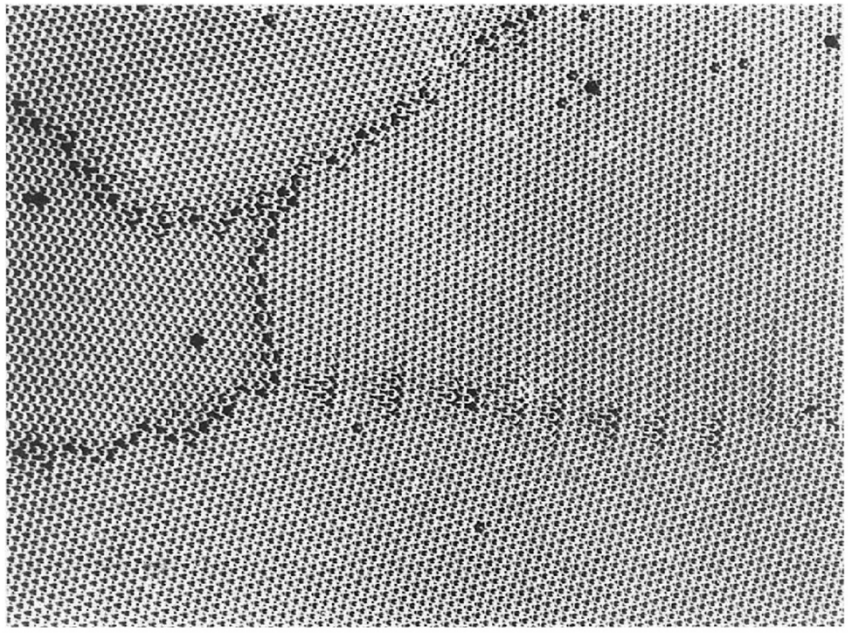

* As disl. glide at low-angle grain boundary
: no change in crystal structure,
just rotation of the lattice into the other grain

Glissile Interfaces between two lattices

Shockley partial dislocation

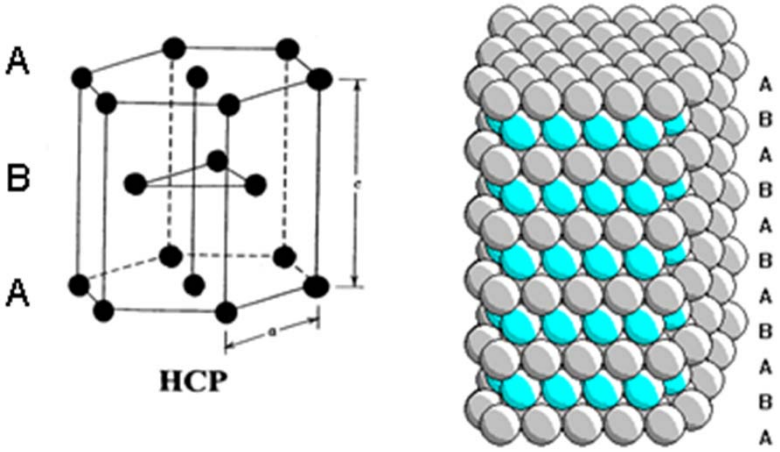

HCP: ABABABAB…

close packed plane: (0001)

close packed directions: $<11\bar{2}0>$

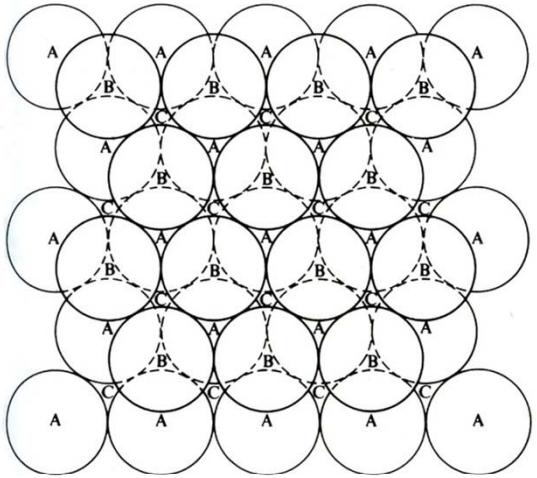

FCC: ABCABCAB…

close packed planes: {111}

close packed directions: $<110>$

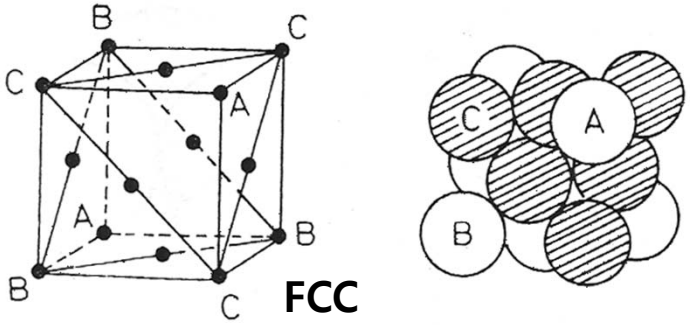

1) Perfect dislocation

$$\vec{b} = \frac{a}{2}[10\bar{1}]$$

In C layer, atoms move

C' → C"

: remain a cubic close-packed arrangement with a fcc unit cell

< FCC → FCC >

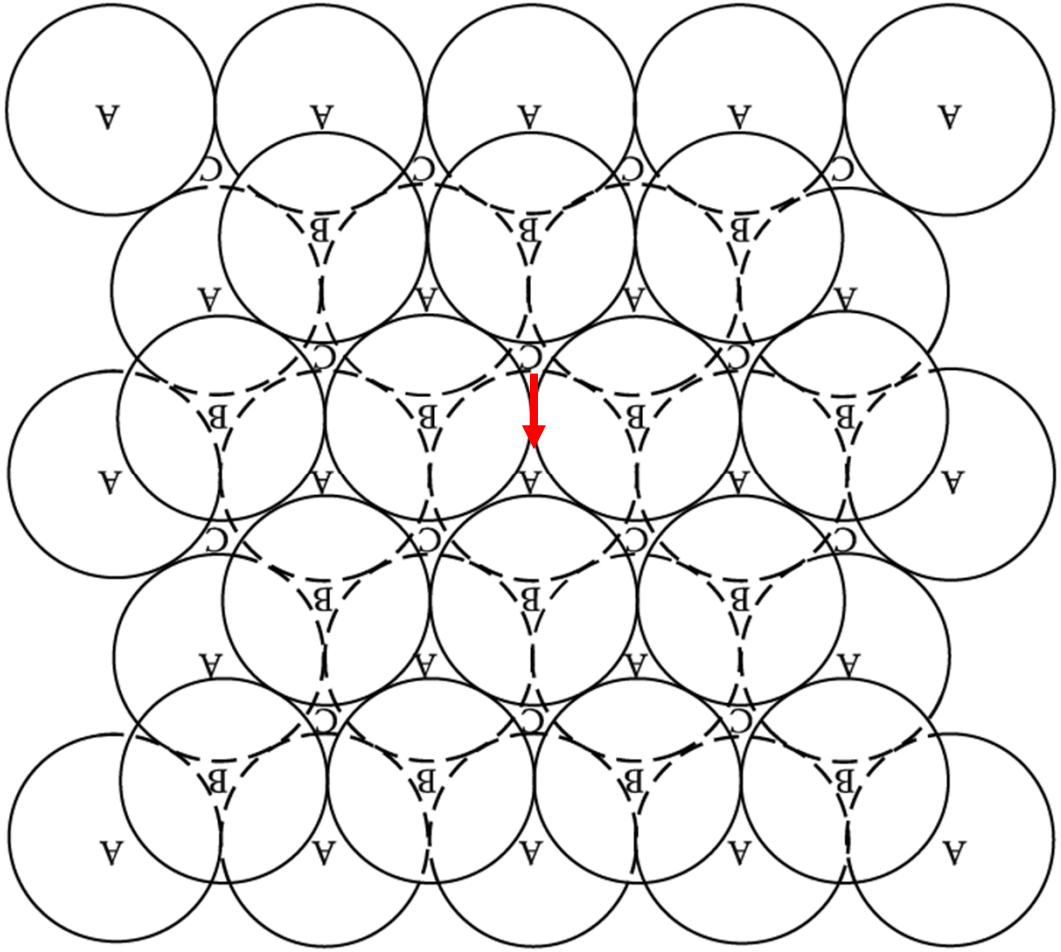

2) Shockley partial dislocation

when atoms move: C' → C"

possible to move C' → A → C"

$$\frac{a}{2}[10\bar{1}] = \frac{a}{6}[11\bar{2}] + \frac{a}{6}[2\bar{1}\bar{1}]$$

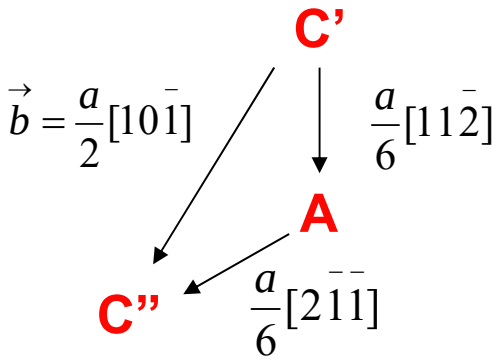

This burgers vector of partial disl. is not located at lattice point.

(can't connect lattice points in the FCC structure)

< FCC → HCP: phase transformation by stacking fault over the area of glide plane swept by the disl.>

Gliding of Shockley partial dislocations ➡ Stacking fault region
적층결함

In thermodynamically stable FCC lattices, the stacking fault is a region of high free energy.
→gliding of partial dislocations : difficult

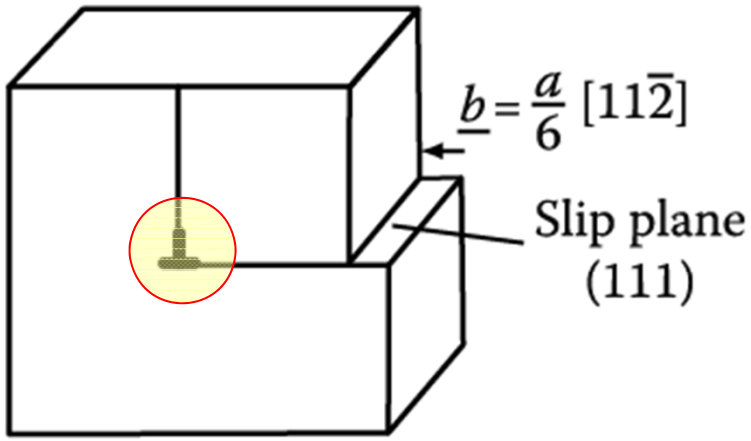

(a)

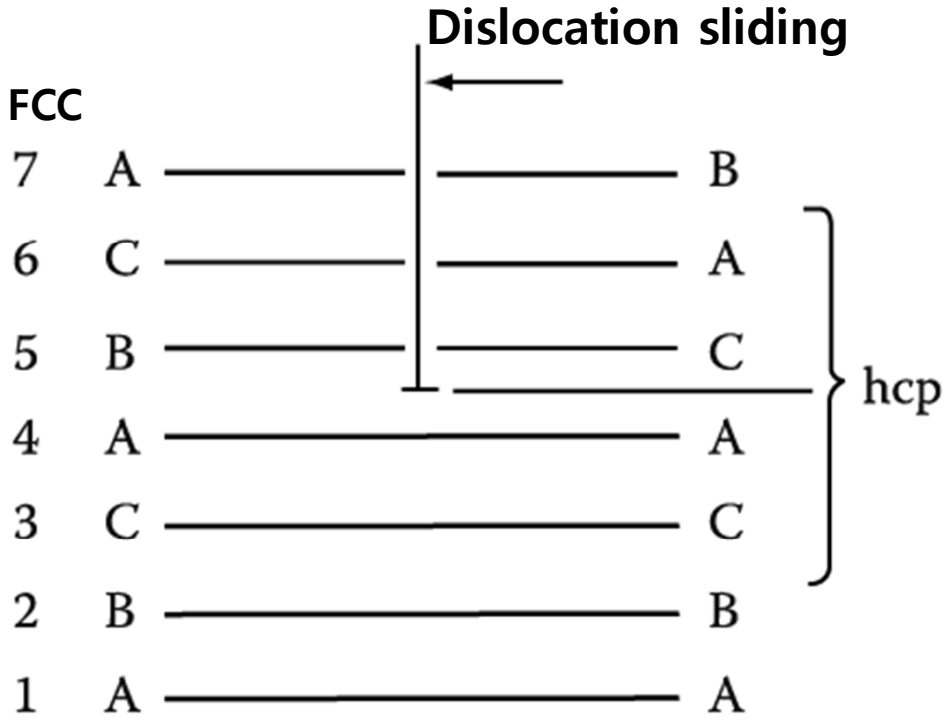

(b)

Fig. 3. 59 (a) An edge dislocation with a Burgers vector b = $\frac{a}{6}$[112] on (11$\bar{1}$). (shockley partial dislocation.)
(b) The same dislocation locally changes the stacking sequence from fcc to hcp.

If FCC lattice is only metastable with respect to the HCP structure → stacking fault E ~ effectively negative → gliding of partial dislocation: easy due to decrease the free energy of system

Glissile Interfaces between two lattices

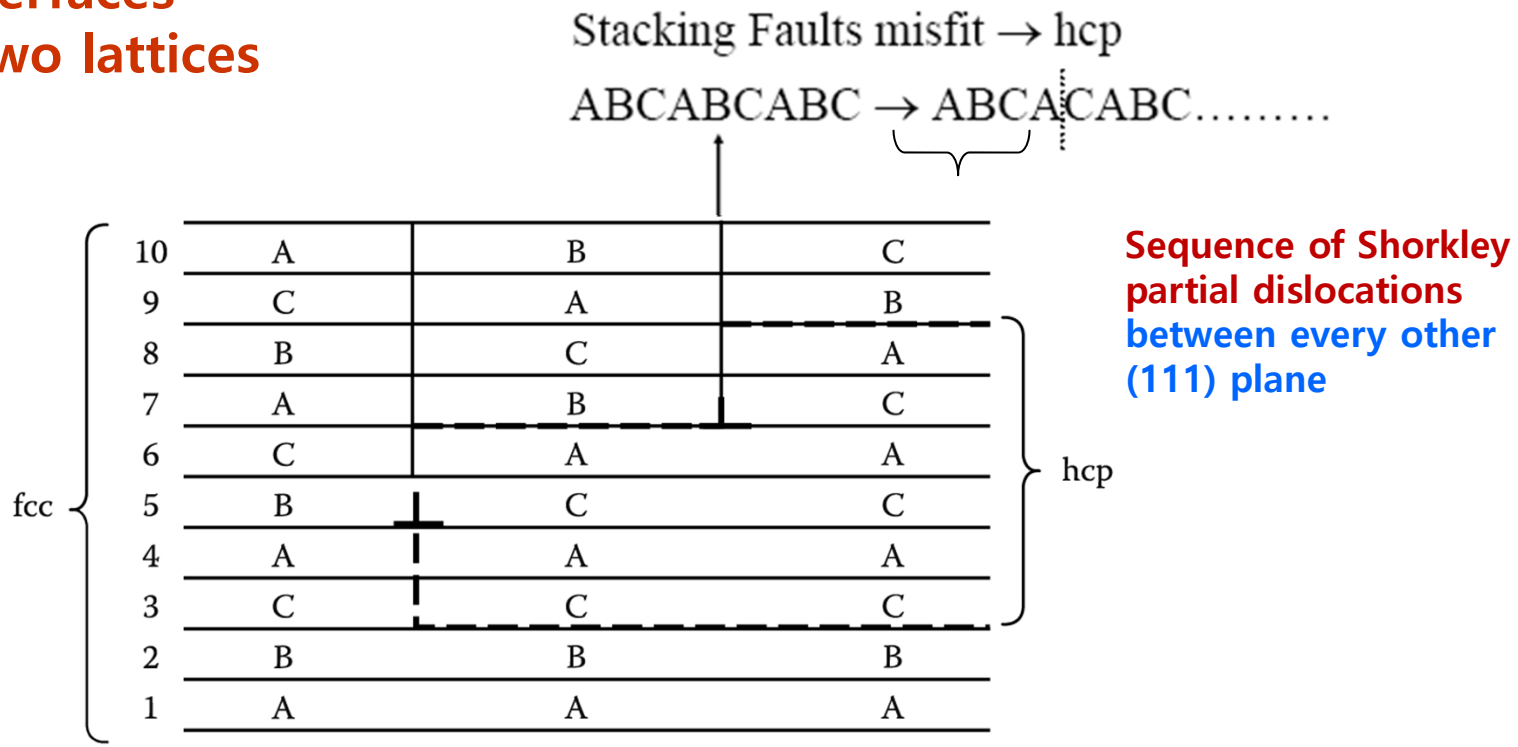

Fig. 3. 60 Two Shockley partial dislocation on alternate (111) planes create six layers of hcp stacking.

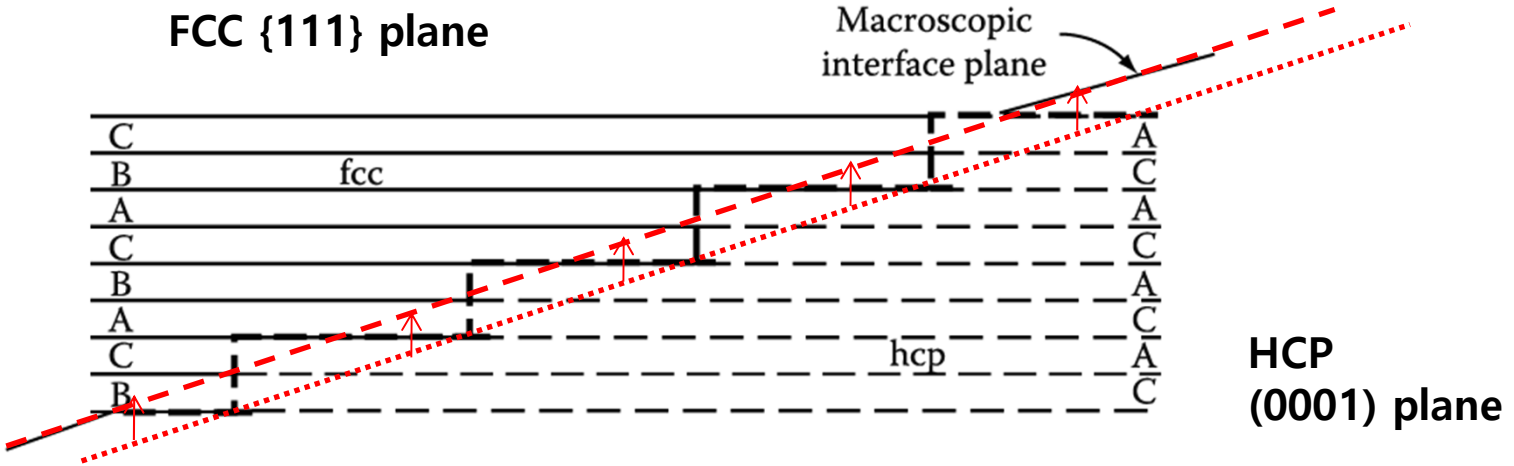

Fig. 3. 61 An array of Shockley partial dislocations forming a glissile interface between fcc and hcp crystals.

An important characteristic of glissile dislocation interfaces
→ they can produce a macroscopic shape change in the crystal.

1) Sequence of same Shorkley partial dislocations between every other (111) plane

→ Pure shear deformation
→ Fcc → Hcp
→ shape change

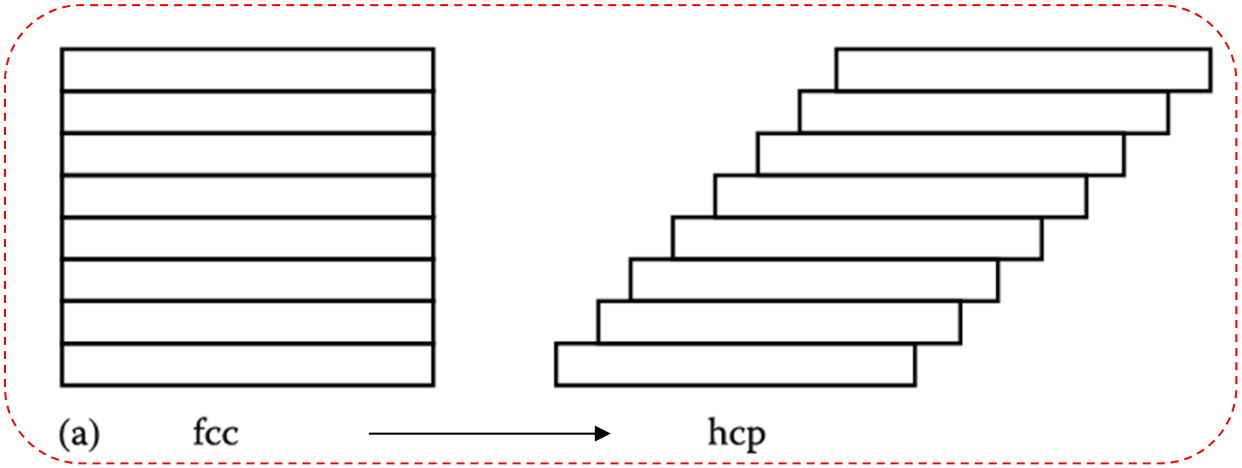

2) If transformation is achieved using all three partials in equal #s,

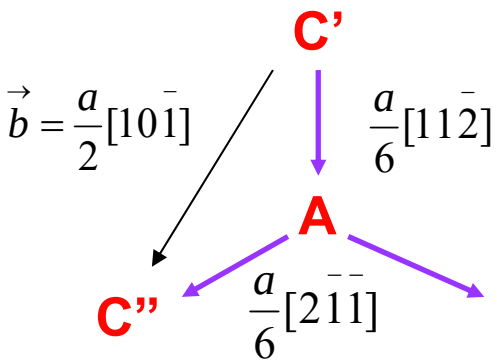

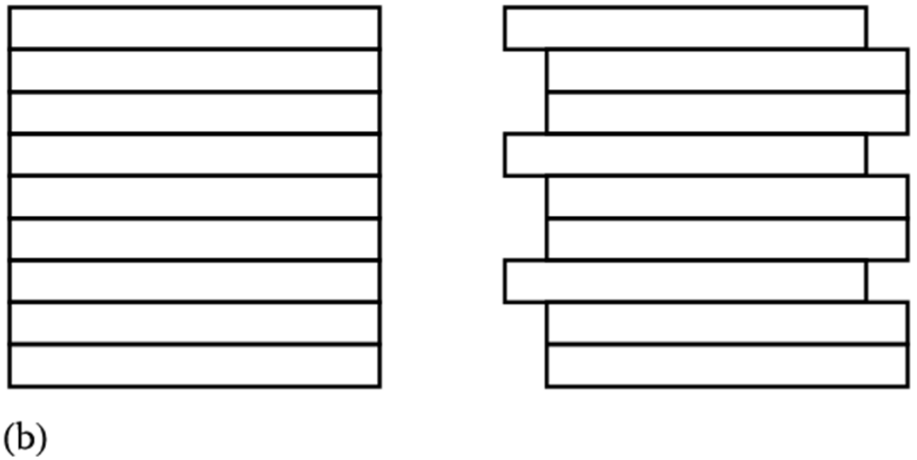

→ No overall shape change

Fig. 3. 62 Schematic representation of the different ways of shearing cubic close-packed planes into hexagonal close-packed (a) Using only one Shockley partial, (b) using equal numbers of all three Shockley partials.

*** Formation of martensite in steel and other alloys:** Motion of Glissile-dislocation interface
: macroscopic shape change & no change in composition
→ more complex interface but same principles (chapter 6)

Contents for previous class

3.4 Interphase Interfaces in Solids

Interphase boundary - different two phases : different crystal structure
different composition

coherent, **Perfect atomic matching at interface**

γ (coherent) = γ_{ch} γ (coherent) ~ 200 mJM^{-2}

semicoherent $\gamma(semicoherent) = \gamma_{ch} + \gamma_{st}$

γ_{st} → due to structural distortions
caused by the misfit dislocations

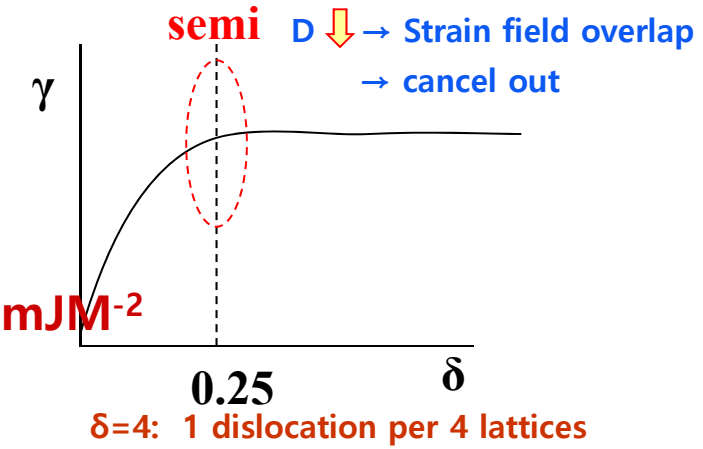

γ(semicoherent) ~ 200~500 mJM^{-2}

incoherent

1) δ > 0.25 No possibility of good matching across the interface

2) different crystal structure (in general)

γ (incoherent) ~ 500~1000 mJM^{-2}

Complex Semicoherent Interfaces

Nishiyama-Wasserman (N-W) Relationship Kurdjumov-Sachs (K-S) Relationships

(The only difference between these two is a rotation in the closest-packed planes of 5.26°.)

The degree of coherency can, however, be greatly increased if a macroscopically irrational interface is formed.

3.4 Interphase Interfaces in Solids

$$\sum A_i \gamma_i + \Delta G_S = minimum$$

Lowest total interfacial free energy
by optimizing the shape of the precipitate and its orientation relationship

Fully coherent precipitates

γ_{ch}

different composition

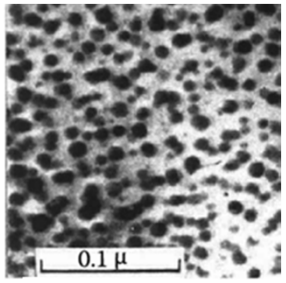

γ_{ch} + ***Lattice misfit*** → γ_{ch} + $Volume\ Misfit\ \ \Delta = \frac{\Delta V}{V}$

Coherency strain energy — Chemical and structural interfacial E

$$\Delta G_S = 4\mu\delta^2 \cdot V \quad \text{(If v=1/3)} \quad \Leftrightarrow \quad \Delta G_S = \frac{2}{3}\mu\Delta^2 \cdot V \cdot f(c/a)$$

Fully coherent precipitates — Incoherent inclusions

$$\Delta G(coherent) = 4\mu\delta^2 \cdot \frac{4}{3}\pi r^3 + 4\pi r^2 \cdot \gamma_{ch}$$

$$\Delta G(non-coherent) = 4\pi r^2 \cdot (\gamma_{ch} + \gamma_{st})$$ → Incoherent inclusions

"Coherency loss"

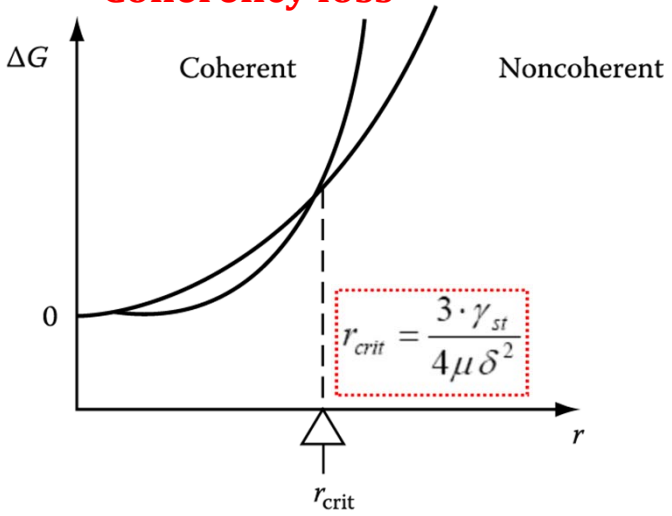

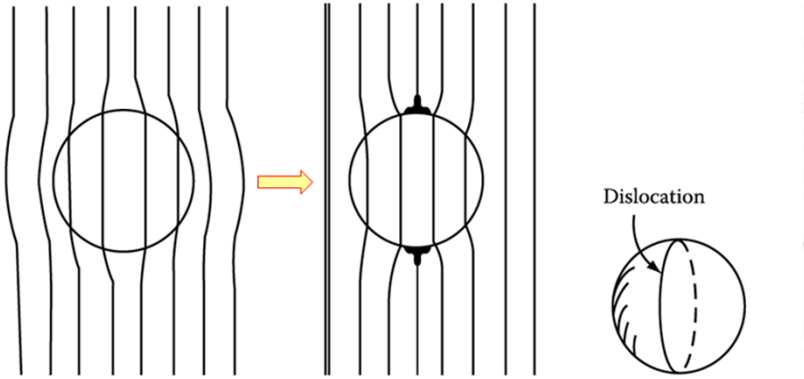

(a) Coherent with strain E (b) Coherency strain replace by dislocation loop. (c) Precipitate with dislocation

3.5. Interface Migration

Phase transformation = Interface creation & Migration

Heterogeneous Transformation (general): parent and product phases during trans.

Nucleation (interface creation) + Growth (interface migration)

Nucleation barrier **Ex. Precipitation**

- at certain sites within metastable alpha phase → new beta phase = Nucleation
- most of transformation product is formed during the growth stage by the transfer of atoms across the moving parent/product interface.

Homogeneous Transformation: PT occurs homogeneously throughout the parent phase.

Growth-interface control

No Nucleation barrier **Ex. Spinodal decomposition (Chapter 5)**

Order-disorder transformation

*** Types of Interface** → **Types of transformation**

- **Glissile Interface: Athermal, Shape change** → **Military transformation**
  Dislocation gliding
- **Non-Glissile Interface: Thermal,** → **Civilian transformation**
  Random jump of individual atoms: extremely sensitive to temp.
  ~ similar way to the migration of a random high angle GB

Classification of Heterogeneous (Nucleation and Growth) Transformation

Type	Military	Civilian			
Effect of temperature change	Athermal	Thermally activated			
Interface type	Glissile (coherent or semicoherent)	Nonglissile (coherent, semicoherent. Incoherent, solid/liquid, or solid/vapor)			
Composition of parent and product phase	Same composition	Same composition	Different compositions		
Nature of diffusion process	No diffusion	Short-range diffusion (across interface)	Long-range diffusion (through lattice)		
Interface, diffusion or mixed control?	Interface control	Interface control	Mainly interface control	Mainly diffusion control	Mixed control
Examples	Martensite twining Symmetric tilt boundary	Massive ordering Polymorphic recrystallization Grain growth Condensation Evaporation	Precipitation dissolution Bainite condensation Evaporation	Precipitation dissolution Soldification and melting	Precipitation dissolution Eutectoid Cellular precipitation

Source: Adapted from Christian, J.W., in *Phase Transformations*, Vol. 1, Institute of Metallurgists, 1979, p. 1.

exception) bainite transformation: thermally activated growth/ shape change similar to that product by the motion of a glissile interface

(need to additional research)